ANALYTICAL APPLICATION OF ION TRANSFER ACROSS THE MEMEMBRANE STABILIZED INTERFACE BETWEEN TWO IMMISCIBLE ELECTROLYTE SOLUTIONS IN A FLOW INJECTION SYSTEM

A Thesis

Presented to the

School of Graduate Studies

Addis Ababa University

In Partial Fulfilment

of the Requirements for the Degree

of Master of Science in Chemistry

by

MULAT ABEGAZ

June 1990

Dedication

TO MY MOTHER

MINTWAB BELETE

Acknowledgement

I pay respect and express my indebtedness to my advisers Dr. B. Hundhammer and Dr. Theodros Solomon whose untiring guidance in every phase of the research made it possible to materialize this work. I would like to express my deep appreciation for their interest in my work and generously gave of their time, energy and valuable advice.

I am also grateful to Dr. S. Wilke from G.D.R for providing me the sample loop. My thanks also go to Daniel Zewge, sister Tabeyin Gedlu and sister Abebech Gedlu who helped me in collecting the blood serum samples and Yemane Asgedom who permitted me to use the flame analyzer for Na and K measurements.

I would like to express my deep gratitude to Yeshi Mekete, Tenagne Bekele, Daniel T/Mariam, Dawit Mengistu Mignote Kassa, Hashim Jemal and Genet Tesfaye who did an excellent typing; printing, part of the drawing, and binding jobs even outside their work time and their moral support and encouragement is also Valuable.

The generosity, moral support and encouragement of colleagues and friends have been invaluable. Special tanks are due to Mr. Demissachew Assefa, Mr. Bekele Bayissa, Hiwot Gedlu, Dr. Eva Zena, staff members of the Ministry of Industry and all who played a role in the realization of this work.

I would also like to acknowledge the Ministry of Industry, for giving me the opportunity to participate in the graduate programme and for various supports.

TABLE OF CONTENTS

List of Tables

List of Figures

Abstract

Using the voltammetric senor which is constracted in our laboratory and the membrane stabilized interface between two immiscible electrolyte solution in a flow injection system the transfer of anions (ClO_4^-, NO_3^- & Cl^-) and cations (K^+ Na^+) from the aqueous to the organic phase have been investigated. In order to determine the working potential region of the system the behaviour of the potential-current dependence of the supporting electrolytes were studied. The iR drop resulting from the dilution effect of the distilled water at the interface has been investigated and it was compensated by increasing the concentration of the supporting electrolyte in the aqueous phase . Dependence of the peak current on the applied potentials and on concentration of various ions (ClO_4^-, NO_3^-, K^+ & Na^+) have been investigated. The determination of K^+ and Na^+ was made in the presence of dibenzo-18-crown-6 in the organic phase. The method was applyed to the determination of Na^+ and K^+ in blood serum samples and the values obtained were in good agreement with the values obtained by flame photometric method. The selectivity of the method was also studied and was found to be potential dependent and governed by the partial sensitivity of the individual ion. A method has also been proposed for the determination of a particular ion in the presence of another ion. The detection limit of the detector has been determined to be about 0.25 μM for perchlorate ion . Thus the method is rapid, precise, sensitive for the determination of some anions and cations.

1.INTRODUCTION

The first review on electrolysis at the interface of two immiscible electrolyte solutions (ITIES) was made by Koryta (1) in 1979, and since then there has been a rapid growth of research activities in both the experimental as well as the theoretical aspect of ITIES (2). The range of applications has also broadened.

Ion transfer across an interface between two electrolyte solution was first studied by Nernst and Riesenfeld as early as in 1902 and Guastalla (3) in 1956.Gaustalla and Gavach (4) then pioneered, in 1968, the use of electrochemical methodology to show that the water-nitrobenzene interface could be polarized. This problem was also studied by Blank (5) and Joos (6,7) who used only one electrolyte and attempted to elucidate the polarization phenomena by different numbers of ions transferred in the aqueous phase (6). The basic properties of the system (ITIES) were widely investigated in 1977 by Koryta, Vanysek and Brezina (8). In their theoretical discussions the conditions where an interface between two immiscible electrolyte solution behaves as an ideal polarized and non-polarizable electrode were discussed.The basic equations for the current-potential dependence at the interface have been deduced for the case of ion as well as electron transfer. These have been further investigated by various groups working in this field, the results of which have been summarized in a number of review articles (1,2,9-17).

Ion transfer across the interface of two immiscible electrolyte solutions has been investigated by several electrochemical techniques such as chronopotentiometry (18-21), cyclic voltammetry and polarography (22-29).

The basic quantity characterizing the equilibria at ITIES is the standard Gibbs energy of partition of individual ions between water to organic solvents. The value of these quantities can be obtained using various extra thermodynamical assumptions. The most frequently us is the tetraphenyl arsonium-tetraphenyl borate (TPAsTPB) assumption of Parker (30) and Popovych (31), which assumes that the standard Gibbs energies of partition of tetraphenyl arsonium cation and tetra phenyl borate anion between any pair of solvents are equal. With this assumption a scale of standard partition Gibbs energies can be calculated for any pair of solvents (28,32-34). A summary of standard Gibbs partition energies and standard Galvanic potential difference is given by Koryta (8,9) for various cations and anions in water/nitrobenzene, water/1,2 dichloroethane and water/1,1 dichloroethane system and by Vanysek (35) in various solvents. The Galvanic potential difference, its components, as well as the relationship and the difference between the Nernst and Donnan equilibria have been discussed by Koczorowski (36) for the case of an interface separating two immiscible electrolyte solutions. Girault and Schiffrin (37) have proposed a new approach for the setting of Galvanic potential scales and ionic Gibbs energies of partition between liquid-phases. Their suggestion was based

on the assumption that the Galvanic potential difference at the potential of zero charge is zero.

The water-nitrobenzene interface has been employed as the main model system in the voltammetric studies of ion transfer made hitherto(38) This is because of the high relative dielectric constant and density value of the solvent, conductivity of its electrolyte solutions and its low solubility in water. However, studies have also been made on the interfaces for example, with water-1,2-dichloroethane (34,38-40), water-acetophenone(41), water-o-nitrophenyloctyl ether(42), water chloroform(11,43), water-dichloromethane (32) and water-organic solvent mixtures (44,45).The mixture of solvents, studied were nitrobenzene + chlorobenzene (41), nitrobenzene + benzonitrile and nitrobenzene + benzene (46). The choice of the organic solvent is based on various factors, among which are solubility of the solvent with water, ion pairing and solvation of ions in the solvent, its influence on the rate of chemical reaction and dielectric constant values of the solvent.

The" potential window", i.e the potential range where the ion transfer of individual ions can be investigated without interference of the transfer of the ions of the base electrolyte, depends on the hydrophilicity of the ions in the aqueous base electrolyte and on the hydrophobicity of the ions of the base electrolyte in the organic phase (9) .The use of tetra butail ammonium tetra phenyl borate (TBA.TPB) as a supporting electrolyte in the organic phase limits the applicable potential range of voltammetric studies by the transfer of tetra butail ammonium (TBA^+) in

the negative potential direction and by the transfer of (tetra phenyl borate) TPB^- to the positive potential side. Thus, transfer only of ions with Gibbs energies of transfer between those of TBA^+ and TPB^- can be investigated/ In order to extend the potential window towards negative potentials tetraphenyl arsonium and crystal violet cations have been used(9). The system with which extremely negative potentials can be reached contains NaF in the aqueous phase and crystal violet in nitrobenzene (28). Further positive potentials can also be obtained by using lithium salts in the aqueous phase and dicarbonyl cobaltate anion in nitrobenzene.

The number of ionic species which can be transferred across the water-nonaqueous solvent interface has so far been limited by the rather narrow range of accessible potential differences between these two phases(2). However, the facilitated transfer of ions like alkali(46,47), and alkaline earth metals(47), Na^+ (21,49-52), K^+ (1,48,52-54), Ca^{+2} (55), H^+ (47,49,52), Li^+ (52, 56) and Cd^{+2}(56) can be made possible in the presence of neutral carriers or ionophores which can form relatively stable complex with a metal ion in the non - aqueous phase. These macrocyclic compounds are uncharged and contain a cavity in which a cation can be embedded. The most known compounds among these are crown ethers which are cyclic polyether compounds with oxyethylene groups CH_2-CH_2-O (57). In 1967, Pederson published his first paper (57) dealing with cyclic polyether compounds. This was followed by other reports (58) dealing with crystalline salt complexes (Na, K, NH_4 , Rb, Cs and Ba

salts) and some new crown ethers (59). Pedersen synthesized some 60 crown ethers (60) which contain from 3 to 10 oxygens in the ring.

The most important application of electrolysis at ITIES has been the determination of standard Gibbs energy of transfer and stability constant of ionophore complexes (9). However, electrolysis at ITIES was applied to the elucidation of the response of ion selective electrodes (57,61-65), the estimation of the rate of the interfacial step of salt extraction(2) and the direct determination of ions(66-69).

The problems connected with the analytical application of the interface between two immiscible electrolyte solutions as a voltammetric sensor are related to the mechanical instability of the liquid/liquid interface and keeping the thickness of the diffusion layer constant (69). Osakai *et al* (69) as well as Marecek and his co-workers (70) solidified the organic phases as PVC-gels, Hundhammer *et al* (69,70) stabilized the liquid/liquid interfaces by inserting a porous membrane between the two liquid phases. The interface is then formed by interfacial tension at the pores of the membrane.

The thickness of the diffusion layer can be kept at a constant value by using a wall jet arrangement of the sensor in a flow system(71). The wall jet electrode was first introduced by Glaurt(72) to describe the flow due to a jet

of fluid which spreads out over a plane surface, the fluid outside the jet being at rest. Wall jet electrode offers high sensitivity and low solution hold up, and thus appears suited for continuous electrochemical measurement in a flowing solution (71). Theoretical explanations, experimental results and the equations for the hydrodynamic boundary layer thickness, the diffusion layer thickness, the limiting current and other parameters have been described and evaluated (71-81), for various solid electrode geometries and wall jet cell arrangement. In some recent work solid wall jet electrodes have been applied for amperometric detection in high performance liquid chromatography (HPLC) (78- 81) and in flow injection system (FIS) (82-84). The application of the wall jet cell to HPLC detector was first reported by Fleet and Little (76) and this technique has been used for the determination of phenols(78). Studies on the dependence of flow rate and column parameter of the amperometric detector response in HPLC, with electrochemical detection have been described (81). FIA technique was first reported by Ruzicka and Hansen(85) in 1975 and this method has been used for the determination of food colouring matters (83), for the determination of diffusion coefficients (84) in a wall jet arrangement of the cell by using amperometric detector.

Hundhammer *et al* (69) and Marecek *et al* (68) have used the membrane stabilized ITIES and the solidified organic phase gel electrode, respectively, for analytical determination, by using a wall jet cell in flow injection system.

The present work deals with the determination of anions (ClO_4^- & NO_3^-)and cations (K^+ & Na^+)across the membrane stabilized ITIES. Specifically sodium and potassium are determined in clinical samples and in water and the results obtained with this method are compared with photometric method. The selectivity as well as the behaviour and the detection limit of the voltammetric sensor are investigated.

2. Theory

The interface between two immiscible electrolyte solution (ITIES), for example between water (W) and an organic liquid (O) has several basic features analogous to the metallic electrode/electrolyte solution interface (1,8,&21). Between the liquid phases there is an electric potential difference. If both phases contain a common uni-univalent electrolyte $B_1 A_1$ then at equilibrium between two phases the electrochemical potential is given by

$$\tilde{\mu}_i(W) = \tilde{\mu}_i(O) \qquad 1$$

$$\mu_i^\circ(W) + RT \ln a_i(W) + zF\varphi(W)$$

$$= \mu_i^\circ(O) + RT \ln a_i(O) + zF\varphi(O) \qquad 2$$

$$\Delta_W^O\varphi = \varphi(O) - \varphi(W)$$

$$= \frac{\mu_i^\circ(W) - \mu_i^\circ(O)}{zF} + \frac{RT}{zF} \ln \frac{a_i(W)}{a_i(O)} \qquad 3$$

$$= \frac{-\Delta_W^O G_{tr,i}^\circ}{zF} + \frac{RT}{zF} \ln \frac{a_i(W)}{a_i(O)} \qquad 4$$

$$= \Delta_W^O\varphi_i^\circ + \frac{RT}{zF} \ln \frac{a_i(W)}{a_i(O)} \qquad 5$$

where the φ_i's are inner electrical potentials, μ_i°s standard chemical potential and a_is activities of the ion i (B_1^+ or A_1^-) in each phase. The quantity $\Delta_W^O G_{tr,i}$ is the standard

Gibbs energy of transfer from the organic to the aqueous phase for the ion i. If equation (5) is summed up for the cation (B_1^+) and anion (A_1^-) as shown below, one can get a further expression for inner electric potentials given by equation (8)

$$\Delta_W^O \varphi = \Delta_W^O \varphi_{B_1^+} + \frac{RT}{ZF} \ln \frac{a_{B_1^+}(W)}{a_{B_1^+}(O)} \qquad 6$$

$$\Delta_W^O \varphi = \Delta_W^O \varphi^o_{A_1^-} - \frac{RT}{ZF} \ln \frac{a_{A_1^-}(W)}{a_{A_1^-}(O)} \qquad 7$$

summing of equation (6) and (7)

$$2\,\Delta_W^O \varphi = \Delta_W^O \varphi^o_{B_1^+} + \Delta_W^O \varphi^o_{A_1^-} + \frac{RT}{ZF} \ln \frac{a_{B_1^+}(W)\, a_{A_1^-}(O)}{a_{B_1^+}(O)\, a_{A_1^-}(W)}$$

but $a_{B_1^+}(W) = a_{A_1^-}(W)$

and $a_{B_1^+}(O) = a_{A_1^-}(O)$

Therefore

$$\Delta_W^O \varphi = \frac{\Delta_W^O \varphi^o_{B_1^+} + \Delta_W^O \varphi^o_{A_1^-}}{2} \qquad 8$$

The above equation was first calculated by Karpfen and Randles (86) in 1953.

2.1. Analogy between ideally polarized ITIES and metallic electrode - electrolyte solution interface.

Let us consider a very hydrophilic salt (A_1B_1) which is practically confined only to the aqueous phase (W) and a very hydrophobic salt (A_2B_2) present in the organic phase (O) Fig 1.

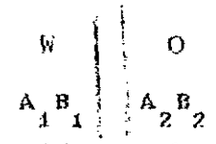

Fig 1 An ideally polarized interface of two electrolyte solution

If a charge is introduced to one of the phases from an external source (and, simultaneously, a charge of opposite sign to the other phase Fig 2) then there exists a potential range (.a potential window) where ITIES behaves like an ideally polarized electrode and the injected charge is used only for double layer charging (1,8,21). The equilibria of the exchange reaction, given by

$$A_1^-(W) + A_2^-(O) = A_1^-(O) + A_2^-(W)$$

$$B_1^+(W) + B_2^+(O) = B_1^+(W) + B_2^+(O) \qquad 9$$

are strongly shifted to the left-hand side and the standard Gibbs energies of transfer of ionic components of the system is given by the following relationship.

$$\Delta^o_W G^o_{tr,B_1^+} + \Delta^o_W G^o_{tr,A_1^-} >> 0$$

$$\Delta^o_W G^o_{tr,B_2^+} + \Delta^o_W G^o_{tr,A_2^-} << 0 \qquad 10$$

The above equations (9) and (10) indicate that the

Equilibria of Interfaces

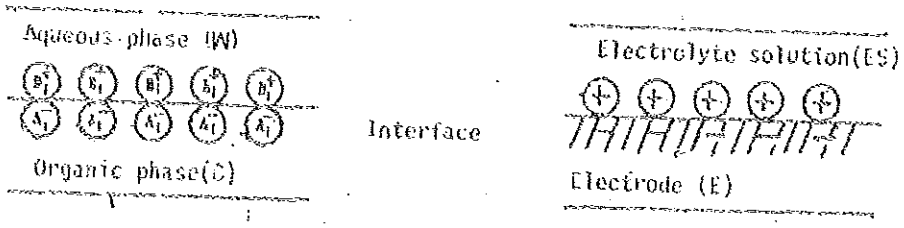

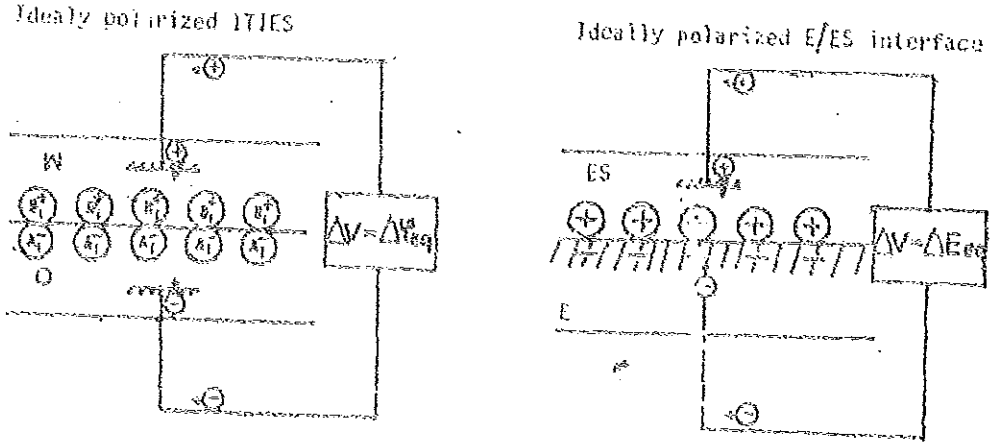

Fig. 2. Charging of Interfaces by External Source(ΔV)

equilibrium distribution of both electrolytes between the solvents W and O is such that the electrolyte A_1B_1 is present almost completely in the solvent W while A_2B_2 is present almost completely in the solvent O. Under these conditions the determination of the potential difference by the activities of the ions present in the system would be difficult since $a_{A_1^-}(O)$, $a_{A_2^-}(W)$, $a_{B_1^+}(O)$ and $a_{B_2^+}(W)$ are very small. Then $\Delta^O_W\varphi_i$ is determined by the charge in the double layer, which can be changed by charging the phases from an external source. This is the condition where the ITIES would be analogous to an ideally polarized electrode (Fig 2). For the case of a metallic electrode/ electrolyte solution interface the charge supplied to or removed from the metallic side are electrons, while in the case of an interface of two immiscible electrolyte only ion transport to and from the interface takes place.

2.2. Current flow across the interface

Let us consider another situation when semi-hydrophobic ions (B_3^+ or A_3^-) are introduced in the previous system (Fig 3)

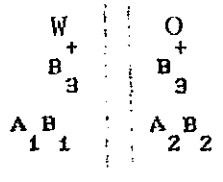

Fig.3 An interface of two immiscible electrolyte solutions under flow of current

at a low concentration. The electrolytes A_1B_1 and A_2B_2 are in excess over the semihydrophobic ions and function as base electrolytes. If a potential difference (ΔV) in excess of

$$\Delta V = \Delta\varphi_{eq} + K \qquad 11$$

the equilibrium potential difference $\Delta\varphi_{eq}$ is imposed on the system from an external source, the charge introduced is used partly for the transfer of B_3^+ across the interface and partly for charging the double layer (Fig 4). The constant term K in the above equation depends only on the composition of the solution of base electrolytes in W and O, on liquid junction potentials and on the reference electrodes but is independent of the nature of the ion B_3^+. The Faradaic current flow across the ITIES is due to a simple charge transfer, which is just analogous to an oxidation reduction reaction at a metallic electrode/electrolyte solution interface (Fig 4).The figures 1-4 are drawn based on Ref.1.

2.3. Analytical application of ITIES

2.3.1 Mechanically stabilized interface

The metal electrode/electrolyte solution interface has been widely used in analytical investigation. However, there are some problems in using the interface between two immiscible electrolyte solutions as a voltammetric sensor in analytical applications, among which the mechanical instability of the interface is the most important one (69). This problem can be overcome by solidifying the organic phases as PVC gels (68) or by inserting a porous membrane between the two liquid phases (69,70)

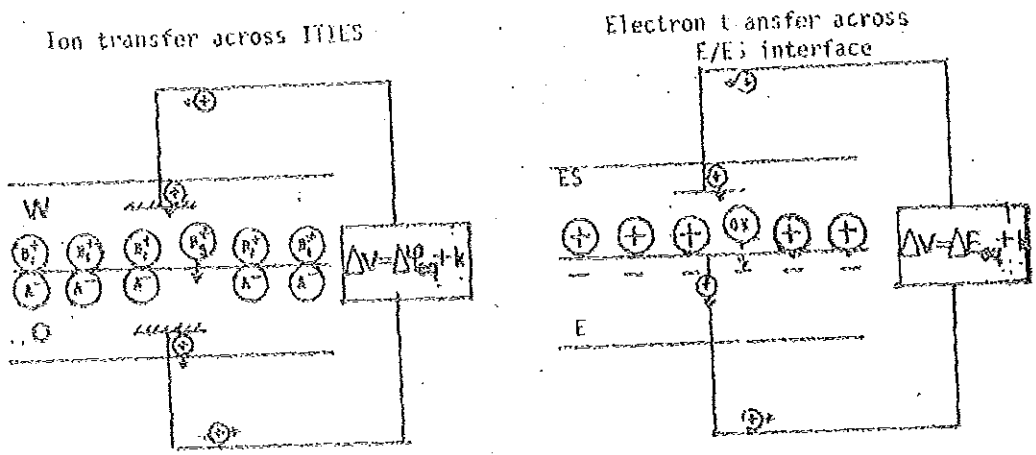

Fig.4.-Charge transfer across interfaces

2.3.2 Constant diffusion layer thickness

The thickness of the diffusion layer can be kept constant by using a wall jet arrangement of the sensor in a flow stream system (71, 73). Wall jet electrode was first introduced by Glauret (72) to describe the flow due to a jet of fluid which spreads out over a plane surface, the fluid out side the jet being at rest. The wall jet may be used as a useful tool in hydrodynamic voltammetry, by allowing a jet of solution issued from a circular nozzle to impinge normally on a disk electrode (indicator electrode) and setting a counter electrode at an appropriate position remote from the wall jet. Such an electrode arrangement is a wall jet electrode (71).

The limiting current attained in hydro-dynamic voltammetry, in which a sample solution is presented continuously to a stationary electrode arises from the establishment of a steady state, constant diffusion layer thickness maintained by the flow of the solution. The magnitude of this current is determined in part, by the geometric factors governing the cell and electrode and by the hydro-dynamic parameters of the flow. Explicit expressions have been derived and verified experimentally in a number of well defined instances (87). Yamada and Matsuda (71) described the limiting diffusion current in terms of the hydrodynamic parameters of the flowing solution by the equation

$$i_l = 1.38nFc^{\circ}D^{2/3}\nu^{-5/12}V^{3/4}a^{-1/2}R^{3/4} \qquad 12$$

This equation defined the performance of the wall jet

electrode in terms of the volume flow rate (V) diameter of the nozzle (a) and radius of the electrode (R), and kinematic viscosity (υ). The same equation was also derived by Gunasinghum and Fleet (78) based on calculation of the hydrodynamic boundary layer-thickness. Equations that relate the diffusion layer characteristics to hydrodynamic parameters are centred on solving the three dimensional equation describing convention diffusion (88)

$$\frac{\partial c}{\partial t} = D\left(\frac{\partial^2 c}{\partial x^2} + \frac{\partial^2 c}{\partial y^2} + \frac{\partial^2 c}{\partial z^2}\right) - \left(V_x\frac{\partial c}{\partial x} + V_y\frac{\partial c}{\partial y} + V_z\frac{\partial c}{\partial z}\right) \qquad 13$$

This equation takes into account the hydrodynamic characteristics of the flowing solution, arising from diffusive mass transfer and from mass transfer due to convective processes.

2.3.2.1 Calculation of the hydrodynamic boundary layer thickness(δ_{bl})

When a fluid flows over a surface, a very thin layer is formed adjacent to the surface in which the velocity gradient normal to the surface is very large. This thin layer is termed the hydrodynamic boundary layer. In this layer the major part of the radial velocity profile is found. According to Glaurt, the radial velocity component (U) is given by the expression.

$$U = \left(\frac{15M}{2\upsilon X^3}\right)^{1/2} f'(\eta) \qquad 14$$

where $\eta = \left(\frac{135M}{92\upsilon^3 X^5}\right)^{1/4} Y \qquad 15$

and X and Y denote distance along, and normal to, the disk wall X being measured from the centre of the disk, υ is the kinematic viscosity and M is the flux of exterior momentum flux, which is constant and can be estimated by the equation (16)

M = 1/2 (typical velocity) (volume flow/radian) 16

η is the radial velocity function which is constant through the whole wall jet and f is the function of distance from the disk surface. If the typical velocity is assumed to be proportional to the mean velocity in a circular nozzle

$$M = 1/2K_1\left(\frac{4V}{\pi a^2}\right)\left(\frac{V^2}{2\pi}\right) = \left(\frac{K_1}{2\pi^3}\right)\left(\frac{V^3}{a^2}\right) \qquad 17$$

where K_1 is proportionality factor, V the volume flow rate of the solution issued from the circular nozzle. Inspection of the radial velocity profiles plotted by using equations defined by Glaurt shows that near the end of the profile $\eta = 6$. This point approximately defines the limit of the boundary layer. Substituting equation (17) in (15) for $\eta = 6$ and simplifying the resulting equation for y (δ_{bl}) one can obtain the equation describing the boundary layer thickness (δ_{bl}) in terms of various hydrodynamic parameters.

$$\delta_{bl} = K_1 \pi^{3/4} a^{1/2} \upsilon^{3/4} x^{5/4} V^{-3/4} \qquad 18$$

2.3.2.2 Estimation of the diffusion-layer thickness (δ_{dl})

For a solution flowing over a body (indicator electrode), there is a region in the immediate vicinity of the surface, where a rapidly changing concentration profile is found,. This region is termed the diffusion layer. According to Levich (78) the thickness of the diffusion layer for flow past a flat plate is given by

$$\delta_{dl} \sim \left(\frac{D}{\upsilon}\right)^{1/3} \delta_{bl} \qquad 19$$

The diffusion layer thickness of the wall jet is then given by

$$\delta_{dl} = k_2 \left(\frac{D}{\upsilon}\right)^{1/3} \delta_{bl} \qquad 20$$

and substituting δ_{bl} from equation (16)

$$\delta_{dl} = K_1' k_2 \pi^{3/4} D^{1/3} a^{1/2} \upsilon^{5/12} x^{5/4} V^{-3/4} \qquad 21$$

2.3.2.3 Derivation of the limiting current equations

From Ficks first law (89) the current due to diffusion-controlled electrolysis is given by

$$i = nFAD \left(\frac{\partial c^{o}(y)}{\partial y}\right)_{y = 0} \qquad 22$$

where A = area of the electrode

y = perpendicular distance to the electrode surface.

The above equation may be simplified to give

$$i_l = \frac{nFADc}{\delta_{dl}} \qquad 23$$

$$= K'nFD^{2/3} c\, a^{-1/2} \upsilon^{-5/12} x^{3/4} V^{3/4} \qquad 24$$

where $K' = \frac{\pi^{1/4}}{K_1 K_2}$

The value of K' was determined experimentally by Gunasinghum and Fleet to be 1.38. Substituting this for K' in eq (24)

$$i_l = 1.38nD^{2/3} C\, a^{-1/2} \upsilon^{-5/12} x^{3/4} V^{3/4} \qquad 12$$

Based on the above relations (equation 12) solid wall jet electrodes have been applied for amperometric detector in liquid chromatography and in flow injection analysis (43) for application which require continuous or automated monitoring. Hundhammer *et al* (69) and Marecek and his co-workers (68) have used the membrane stabilized ITIES and the solidified organic phase gel electrodes, respectively for analytical determination by using the same relation given in equation(10).

2.4. Facilitated ion transfer

2.4.1 The need for facilitated ion transfer

The narrow range of accessible potential differences (potential window) between the two phases is another problem which can limit the number of ionic species transferred across the interface. However, the transfer of some ions like alkali and alkaline earth elements can be facilitated

by the presence of ionophores (neutral carries) in the organic phase.The principle of ionophore-facilitated ion transfer was first described by Koryta (1). An ionophore is a strongly hydrophobic particle which possesses acceptor properties for ions or which is a complex former or a proton acceptor. The ionophore-ion associate must be also hydrophobic.The investigation of ionophore-facilitated ion transfer can be carried out in two ways. In the first case the concentration of the metal cation in the aqueous phase is considerably higher than that of the ligand in the nitrobenzene phase. Under these conditions, the peak or limiting current is proportional to the ligand concentration in the nitro-benzene phase. In the second case the concentration of ligand in the organic phase is considerably higher than that of the metal cation in the aqueous phase. Under these conditions the peak or limiting current is proportional to the metal cation concentration in the aqueous phase.

2.4.2 Mechanism

The way in which the strong hydrophobic ionophore L mediates the translocation of the metal cation M from the aqueous (W) to organic (O) phase can be described as the formation of the complex between M^+ and L (47)

$$M^+(W) + L(O) = ML^+(O)$$

the steps which may be involved are the partition reaction

$$M^+(W) = M^+(n)$$

followed by the formation or dissociation of the complex in the bulk of the organic phase, i.e.

$$M^+(O) + L(O) = ML^+(O)$$

In equilibrium we have

$$\Delta^{W}_{O}\varphi = \Delta^{W}_{O}\varphi^{\circ}_{M^+} + \frac{RT}{ZF} \ln \frac{[M^+(O)]}{[M^+(W)]}$$

or in terms of the stability constant K_{ML} where:-

$$K_{ML} = \frac{[ML^+(O)]}{[M^+(O)][L(O)]}$$

$$\Delta^{W}_{O}\varphi^{\circ}_{M^+} = \Delta^{O}_{W}\varphi^{\circ}_{M^+} + \frac{RT}{ZF} \ln \frac{[ML^+(O)]}{[L(O)]\ K_{ML}[M^+(W)]} \qquad 25$$

3. Experimental

Figure 5 shows the scheme of the experimental set up used as a flow injection system. The wall-jet electrochemical cell employed is shown in Fig 6.

The variable voltage source, an amperometric detector and the four electrode potentiostat with iR drop compensation were constructed in the laboratory and all of them were tested employing an electrical equivalent of ITIES (Dummy cell) before, using them in the flow system at ITIES.

3.1. Construction of the variable voltage source:-

The variable voltage source was constructed by using Zener diodes as a voltage stabilizer (90). This source was constructed (Fig 7) to give a variable voltage ranging from +2V to -2V and the required voltage could be adjusted by the help of a polarity switch and a 50k ohms multiturn potentiometer. Each turn of the 10 turn potentiometer was calibrated using a digital multimeter (Tektronix Model DM501) and the results are indicated in table 1. The lay out of the variable voltage source is shown in Fig 8.

Fig.5. Block diagram of the flow-injection system

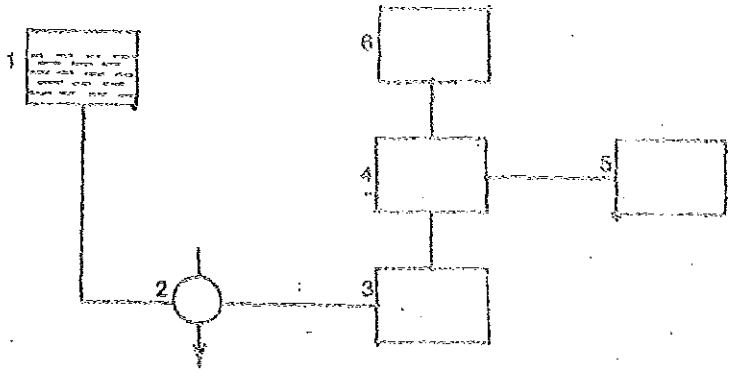

1. Reservoir of the carrier- solution, 2. Sample loop, 3. Detector,
4. Four electrode potentiostat, 5. Variable voltage supply, 6. Y-t recorder.

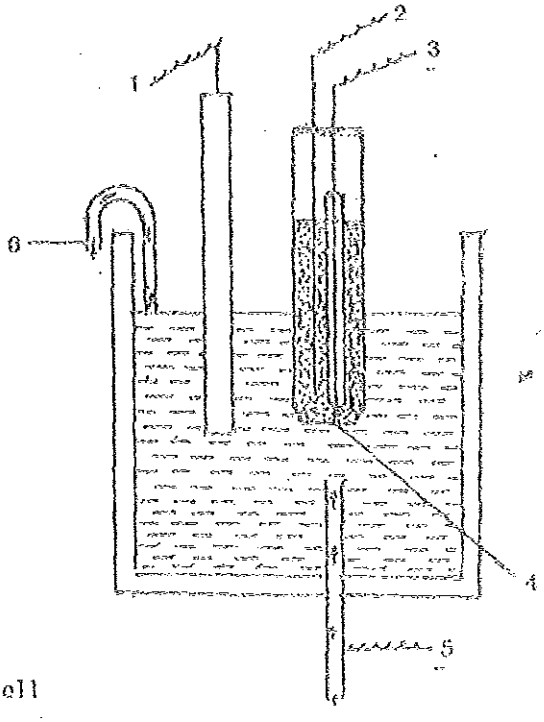

Fig.6. Wall jet cell

(1), (3) Reference electrode, (2) counter electrode in the organic phase,
(4) membrane, (5) jet inlet (stainless steel needle) serves as counter electrode, (6) out let.

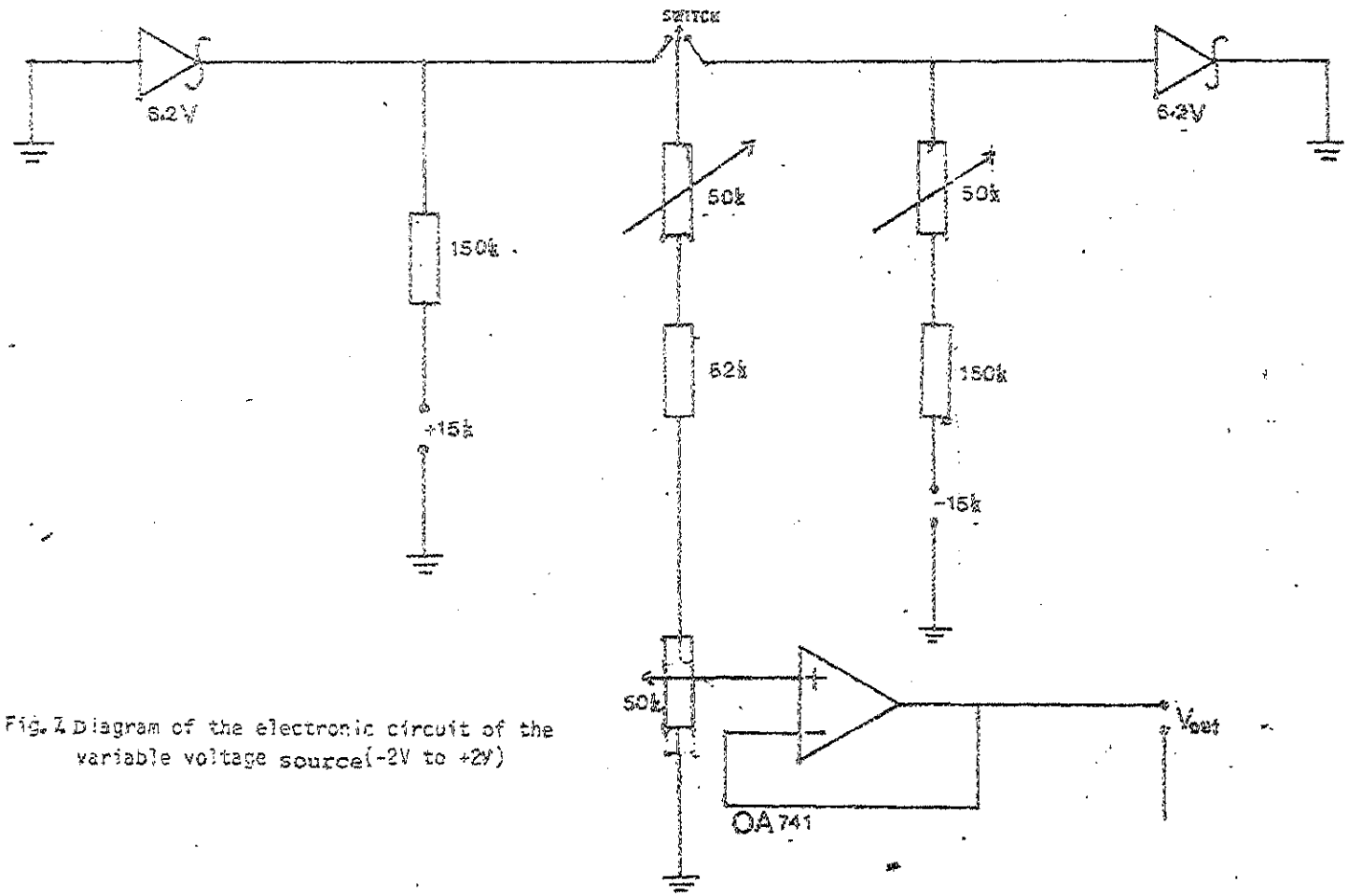

Fig. 4 Diagram of the electronic circuit of the variable voltage source(-2V to +2V)

Table 1. The volatage obtained for each term of the potentiometer. The readings were taken from a digital multimeter.

No.of turns	postive polarity (V)	negative polarity(V)
0	0.032	0.026
1	0.230	0.224
2	0.427	0.422
3	0.624	0.619
4	0.821	0.817
5	1.018	1.044
6	1.216	1.213
7	1.414	1.411
8	1.611	1.608
9	1.808	1.806
10	2.004	2.003

The mean voltage difference between two consecutive terms is 0.1972 for postive polarity and 0.1977 for negative polarity and the standard deviation is 0.7071mV for postive polarty and 0.6749mV for negative polarity

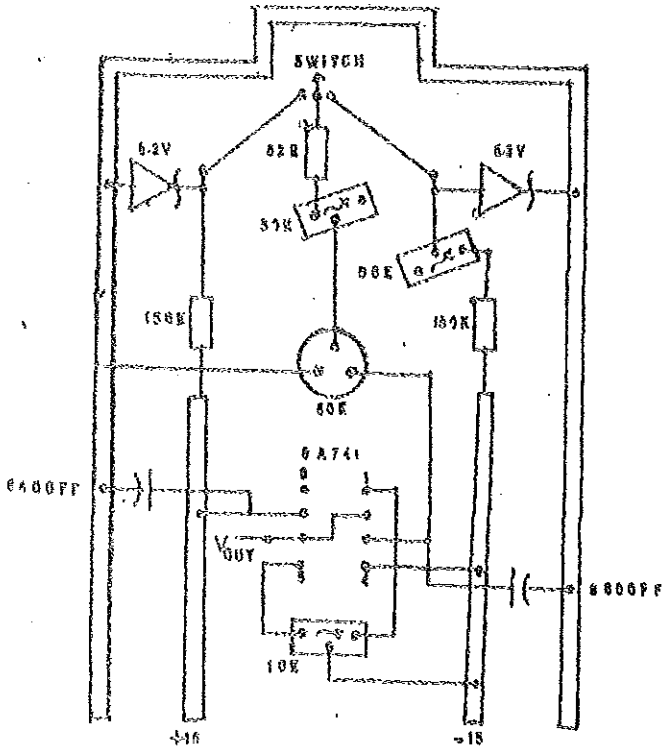

Fig.8. The lay out of the variable voltage source (-2V to + 2V)

3.2. Construction of the amperometric detector and the four electrode potentiostat with iR drop Compensation.

A potentiostat is an important device which automatically maintains the working electrode potential at a chosen (programmed) value irrespective of the current passing through the electrolytic vessel(91). The potentiostat used for the experiment was constructed by using the electronic circuit diagram (46) shown in Fig 9. The potentiostat is represented by the operational amplifiers OA 1-3. When the voltage from the variable voltage source is applied to the summing input of the potentiostat, the same voltage of the opposite sign appears at the contact to the reference electrode RE(W) while the contact to the reference electrode RE(0) is always held at virtual ground. Because each reference electrode is connected to the high impedance input of the operational amplifier (OA2 or OA 3) only a negligible current can flow through each of them. The current flowing through the interface is supplied by the outputs of the operational amplifiers OA1 and OA3 by means of the counter electrodes CE(W) and CE(W) and CE(0). Its value can be measured as the floating voltage drop across the resistor R . The variable resistor R can have a value of 1 K, 10 K, 100 K or 1000 K Ohms and these are connected by the help of a switch, so that a shift from a lower voltage to higher voltage or vice-versa would be possible.For our experiment 10 K ohm

Fig.

resister was used for all measurements. The combination of the operational amplifiers OA 4-6 were used to convert the floating voltage drop into a voltage versus ground. The out put of the operational amplifier OA6 was connected to the input of a Yt recorder (Pedersen model 27MR) to record the output voltage against time, or to a digital pH meter (Philips PW 9409) to record the voltage. This voltage is proportional to the current flowing through the interface. By the help of a positive feedback a part of this voltage is fed back to the potentiostat, which can be adjusted by the help of a 10 K ohms multiturn potentiometer. This voltage is exactly equivalent to the iR voltage drop resulting from the resistance of the solution. The iR drop compensation was set to the nearest point before oscillation. The layout of the amperometric detector and the four electrode potentiostat with iR drop compensation is shown in Fig 10.

3.3. The flow system and the sample loop

The flow system was realized by utilizing a gravity flow. A container filled with a carrier solution (supporting electrolyte of the aqueous phase) was positioned at the required height and the solution was made to pass through the tubing to the sample loop. A 2.5 meter stand was made to adjust the required height. Using this adjustment a flow rate ranging from 2-5 ml/min can be

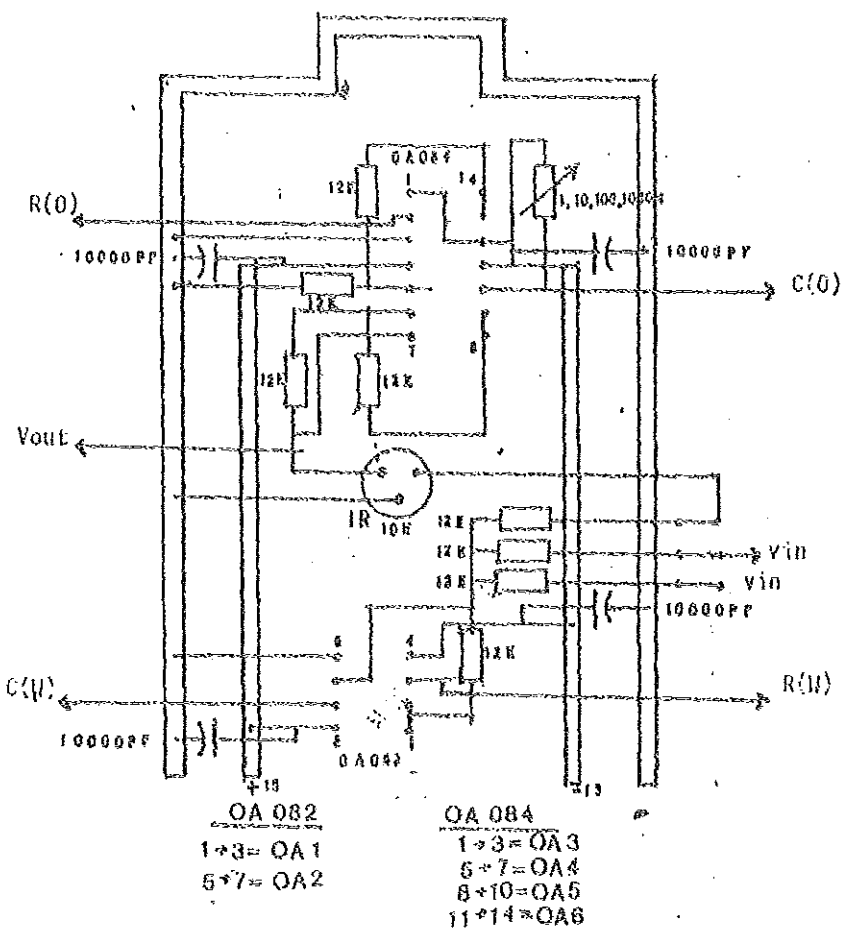

Fig.10. The lay out of the four electrode potentiostat with iR drop compensation and the amperometric detector.

obtained. For our experiment a flow rate of 3.2 ml/min was used for all measurements. A sample loop which can inject 25 μl sample solution to the carrier stream was made by S. Wilke and his generous gift is gratefully acknowledged. In order to see the relative position of the jet of solution to the interface and how this solution impinge on the surface of ITIES, a jet of coloured solution (a solution of potassium permanganate) was injected to a stream of colourless carrier solution.

3.4. Wall jet electrochemical cell

The wall jet electrochemical cell arrangement is shown in Fig 6. Two auxiliary electrodes (one platinum wire for the organic phase and the other one a stainless steel needle which was also the jet inlet in the aqueous phase) served as source and drain of current while the potential difference across the interface was controlled by means of two reference electrodes. The reference electrode in the aqueous phase was Ag/AgCl/KCl sat'd whereas a silver wire electrode was used in the organic phase. The tip of this reference electrode was placed near to the interface.

A hydrophilic acetyl cellulose membrane (PT325) having a thickness of 45 μm was used to stabilize the water /nitrobenzene interface. A disk of this membrane, 1.5 cm in

diameter was fit onto a glass tube (inner diameter 0.6 cm) by the help of a plastic O-ring.The glass tube was filled with 10 mM solution of CV-TPB in nitrobenzene which was used as a supporting electrolyte in the organic phase. The supporting electrolyte in the aqueous phase was 100 mM solution of $MgSO_4$.

In order to compare the results obtained by the voltammetric censor with the flame photometric method a Gallenkamp Flame Analyser FGA-330 was used for the determination of Na and K in blood serum samples.

The chemicals were of analytical grade and were used without further purifications. The CV-TPB was prepared by mixing equimolar amounts of CVCl and NaTPB, both dissolved in methanol and the resulting mixture was diluted with distiled water. The precipitate of CV-TPB was filtered off and washed with distiled water until a test for chloride in the filtrate was negative.

Stock solutions were prepared at a concentration of 0.1 M for all the studied electrolytes, and were diluted with redistilled water as necessary. The measurements were made at a laboratory temperature of $22 \pm 2^{\circ}C$

Table 2 Cost break down of the instrument

1. Four Electrode Potentiostat

Items		Stock No	Qty	Price (£)
1. High stability carbon film				
0.5 w resistors	12 KΩ	132-753	8	0.208
	1 KΩ	132-494	1	0.026
	10 KΩ	132-731	1	0.026
	100 KΩ	132-977	1	0.026
	1 MΩ	133-217	1	0.026
2. Multiturn helical potentio-meter				
10 turn	10 KΩ	173-518	1	8.640
3. Polystyrene capacitors				
10,00 PF		113-409	4	0.580
4. BIFET Op-amps TL082CA(dual)		304-217	1	1.050
" " TL084ON(quad)		304-201	1	1.770
5. d.i.l aplifier sockets				
'8 ways		401-683	1	0.526
d.i.l amplifier	14 ways	401-655	1	0.640
6. 4 mm insulated terminals		412-201	2	1.060
7. Banana plugs		444-179	2	0.414
8. 'bnc' plugs		455-624	4	4.880
9. 'bnc' sockets		455-674	4	4.880
10. H.B.C. (main fuses)		414-257	1	0.520
11. 15A Toggle S.P.ST.T.		316-822	1	1.310
12. 11 turn analogue dial mechanism		508-885	1	8.300
13. MIDG W/C SW 1pole 12 way		327-642	1	0.680
14. Control knobs 3/4 in		499-040	1	0.746
15. Knob skirts 3/4 in		499-832	1	0.392

Items	Stock No	Qty	Price (£)
16. Encapsulated fixed voltage power supply -15 V/240 V	591-124	1	44.470
17. miniature cable	367-280	3 m	0.6504
18. Laminated sheet (10x15x3.2)	433-523	1	0.453
19. Metal casesstandard (204x152x76)	501-828	1	0.453
20. Moulded plug and socket	487-031	1	2.800
21. Silicon rubber wire	359-627	3 m	0.391
22. Miniature standard wire	357-334	3 m	0.071
Total	-	-	99.095

2. Variable Voltage Source (-2v + 2v)

Items		Stock No.	Qty	Price (£)
1. High stability carbon film resistors	150 KΩ	133-015	2	0.052
	82 KΩ	132-955	1	0.026
2. Cermet trimmer	50 KΩ	162-259	2	1.500
	10 KΩ	162-237	1	0.750
3. Multiturn helical potentiometer		173-530	1	8.640
10 turn	50 KΩ	173-530	1	8.640
4. Polystyrene capacitors 6800 PF		113-386	2	0.290
5. Zener diode BZY88 series 6.2 V (500 mw)		282-101	2	0.240
6. LM725 On Instrumentation		305-311	1	0.358
Amplifiers 741		282-101	1	0.358
7. d.i.l amplifier sockets 8 way		401-683	1	0.526
8. 11 turn analogue dial mechanism		508-885	1	8.300
9. Laminated sheet(10x15x3.2mm)		433-523	1	0.453
10. 4mm insulated terminals		423-201	3	1.590
11. Banana Plugs		444-179	3	0.621
12. Silicon rubber wire		359-627	2 m	0.261
Total		-	-	23.507

Total Sum 122.602(Birr 392)

The cost of the instrument which contains the variable voltage source, the amperometric detector and the four electrode potentiostat with iR drop compensation was calculated and it was about £125 (Birr 400). This cost includes all electronic components, casing, sockets, plugs cables control knobs, switches etc. See Table 2 for the cost break down of the instrument. The picture of the instrument is shown in Fig 11.

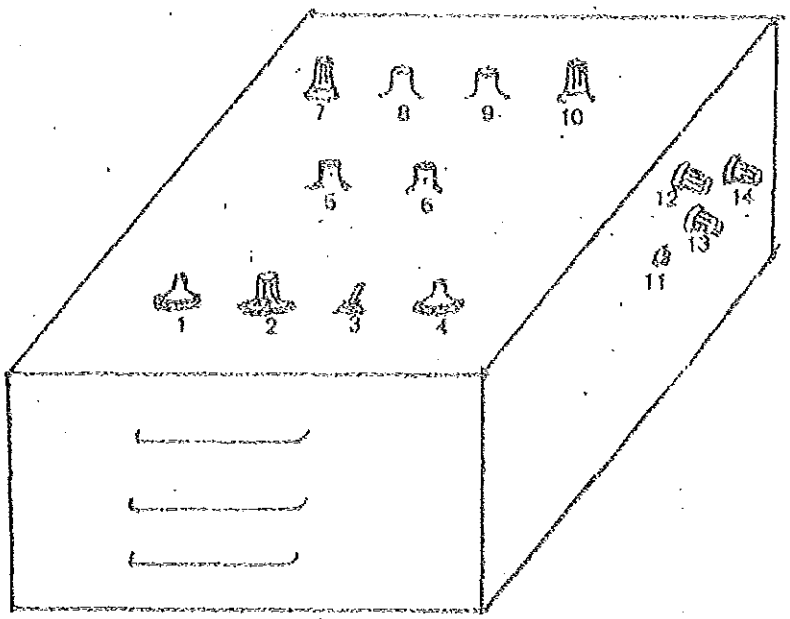

Fig.11 The picture of the instrument

1. IR drop Compensation
2. Variable Resistor
3. Polarity Switch
4. Variable Voltage Source
5. Output
6. Input
7. Reference Electrode Organic Phase
8. Counter " " "
9. Counter Electrode Aqueous Phase
10. Reference " " "
11. Variable Voltage Mode
12. Ground
13. +15 Volt Mode
14. -15 Volt Mode

4. Results and Discussion

4.1. General Aspects

Using the membrane stabilized ITIES the transfer of anions (ClO_4^-, NO_3^- & Cl^-) and cations (K^+ & Na^+) from the aqueous to the organic phase have been investigated.

4.1.1 The behaviour of the supporting Electrolyte.

The potential current curve shown in Fig 12 was obtained for the electrolyte 10 mM CV-TPB in nitrobenzene and 10 mM $MgSO_4$ in water. This curve was obtained as follows.The potential was changed in steps of 20 mV At each potential the current output from the potentiostat was monitored on a digital pH meter The current was then plotted versus potential From this curve (Fig 12) the working potential region of the system can be determined. The sharp increase in the curve at the positive potential end may be due to the transfer of Mg^{+2} from the aqueous to the organic phase or of TPB^- from the organic to the aqueous phase. At the negative potential end the sharp decrease may due to the transfer of SO_4^{-2} from the aqueous to the organic phase or CV^+ from the organic to the aqueous phase. Therefore the working regions of the sensor i.e. the determination of other ions would be limited between the two ends of the curve where the transfer of the ions supporting electrolyte becomes negligible.

-0.28
-0.24

4.1.2 Effect of redistilled water on the resistance of the solution.

In flow injection analysis, the axial concentration profile of the ion being investigated, which is caused by dispersion of the injected sample in the laminar flowing carrier stream, was monitored by the current time response. This is shown in Fig 13 and 14, when a 25 μl sample solution of 1 mM $NaClO_4$ was injected into a carrier solution of 10 mM MgSO4. Fig 13 was obtained as a result of the transfer of ClO_4^- and Fig 14 due to the transfer of Na^+ across the interface from the aqueous to the organic phase in the presence of neutral carrier dibenzo 18-crown-6 (DB-18-C-6) in nitro benzene.The detector response shown in Fig 13 and 14 were at a potential ($\Delta^o_w E$) of 30 mV and 350 mV respectively.

The downward spike for the cation shown in Fig 14 was observable for concentrations below 0.5 mM, though the height of the spike was low at high concentration and high at low concentration. In addition to this anomalous peak, the peak currents obtained for lower concentration of anions (< 1 μM) were almost equivalent. In order to investigate this anomalous situation redistilled water was injected into the carrier stream. A peak which is equivalent to the peak currents obtained for lower concentration (< 1μM) of anions were obtained, and this has an effect on the detection limit of the detector. When the peak currents (ip) of these peaks were plotted against the applied potential difference, Fig 16 was obtained. The effect of

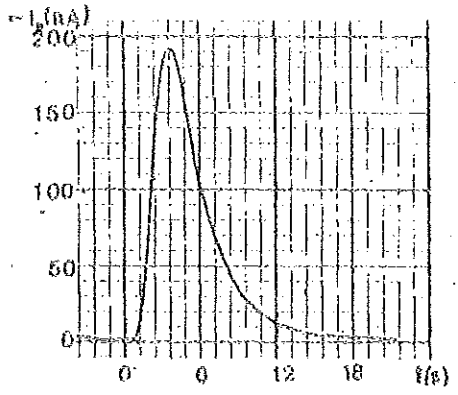

Fig 13

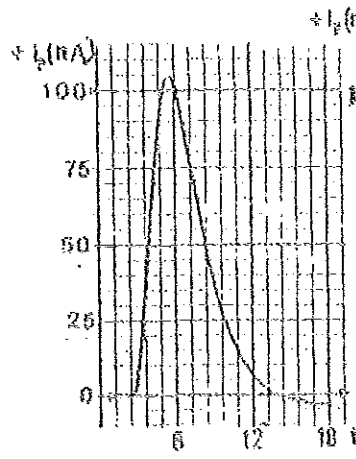

Fig 15

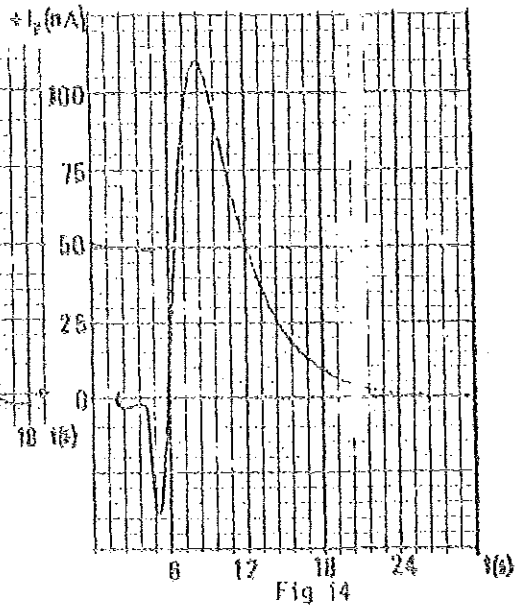

Fig 14

Fig.13,14 and 15. Detector response to an injected sample of $NaClO_4$. Fig 13 for ClO_4^- and Fig 14 for Na^+ in 10mM $MgSO_4$ and Fig 15 for Na^+ in 100 mM $MgSO_4$ (supporting electrolyte in the aqueous phase) and the supporting electrolyte in the organic phase 10 mM CVTPB and 10 mM DB-18-C-6 as neutral carrier.

Fig.16. Depe
elec

redistilled water on various concentration of the supporting electrolyte was studied. The current peak was low for high supporting electrolyte concentration and almost negligible for the concentration of the supporting electrolyte grater than 100 mM $MgSO_4$. The possible explanation for these observation is given below.

Under normal condition the total applied potential(E_{ap}) to the cell consist of the working potential (E_W) of the cell and a potential drop through the solution owing to its resistance (iR).

$$E_{ap} = E_W + iR \qquad 26$$

The iR voltage drop can be compensated by the positive feed - back of the four electrode potentiostat as shown in Fig 9 section 3.2. When a jet of redistilled water is injected into the carrier stream of the supporting electrolyte (10 mM of $MgSO_4$) the resistance of the solution will increase at the ITIES due to the dilution of the carrier solution at the interface.

This leads to a change in iR drop and this potential drop would be a maximum when the maximum amount of redistilled water reaches the interface, as a result a peak current would be obtained. This current can be a capacitive (charging) current, since it is not a result of ion transfer

and it can be given by

$$\frac{\partial}{\partial t}\left(E_{ap} - E_{W} \right) = \frac{\partial \Delta E}{\partial t} = i_c R \qquad 27$$

Multiplying both sides by a constant C(capacitance)

$$C \frac{\partial \Delta E}{\partial t} = i_c RC$$

but $$C\Delta E = q \qquad 28$$

$$\frac{\partial q}{\partial t} = i_c RC$$

$$i_c = \frac{1}{RC} \frac{\partial q}{\partial t} \qquad 29$$

The charging current i_c increases with potential and reaches a maximum value at the -ve and +ve ends of the applied potential as shown in Fig 16. The amount of charging current would be minimized if the concentration of the supporting electrolyte increases, for example 100 mM of $MgSO_4$. At this concentration the dilution effect of redistilled water is minimized. Fig 15 shows the detector response to an injected sample of Na^+ in the presence of neutral carrier (DB-18-C-6) in the organic phase when the concentration of the aqueous supporting electrolyte was 100 mM $MgSO_4$ ($\Delta^{O}_{W}E$ was the same as in Fig 14 .)

4.1.3 Dependence of peak current on the applied potentials.

When the output current maximum (ip) as shown in Fig 13, 14 and 15 was plotted against the applied potential difference ($\Delta_w^o E$) Fig 17 is obtained for 0.1 mM ClO_4^- and 0.1 mM NO_3^- .Tables 3,4 and 5 compiles the values of (ip) obtained for other concentration of these anions and for Cl^-. As shown from the diagram and the tables , when the applied potential ($-\Delta_w^o E$ or $+\Delta_w^o E$) increased over a particular potential range, the peak current increases, due to the transfer of anions (-ve current) and cations (+ve current) across the interface from the aqueous to the organic phase. Subsequent to this potential range, a region is reached where the current is independent of the potential and has a limiting value which is the limiting current. This limiting current depends on the concentration of the ion being transferred across the ITIES . As a result an S shaped i-E curve as shown in Fig 17 is obtained.

One of the most important parameter from Fig 17 is the half wave Galvani potential difference $\Delta_w^o \varphi_{1/2}$ which is given by

$$\Delta_w^o \varphi_{1/2} = \Delta_w^o \varphi_t + \frac{RT}{2ZF} \ln \frac{D^o}{D^w} + \frac{RT}{ZF} \ln \frac{\gamma^w}{\gamma^o} \qquad 30$$

This is a potential on a polarographic curve at which the current reaches half of its limiting value, and mainly

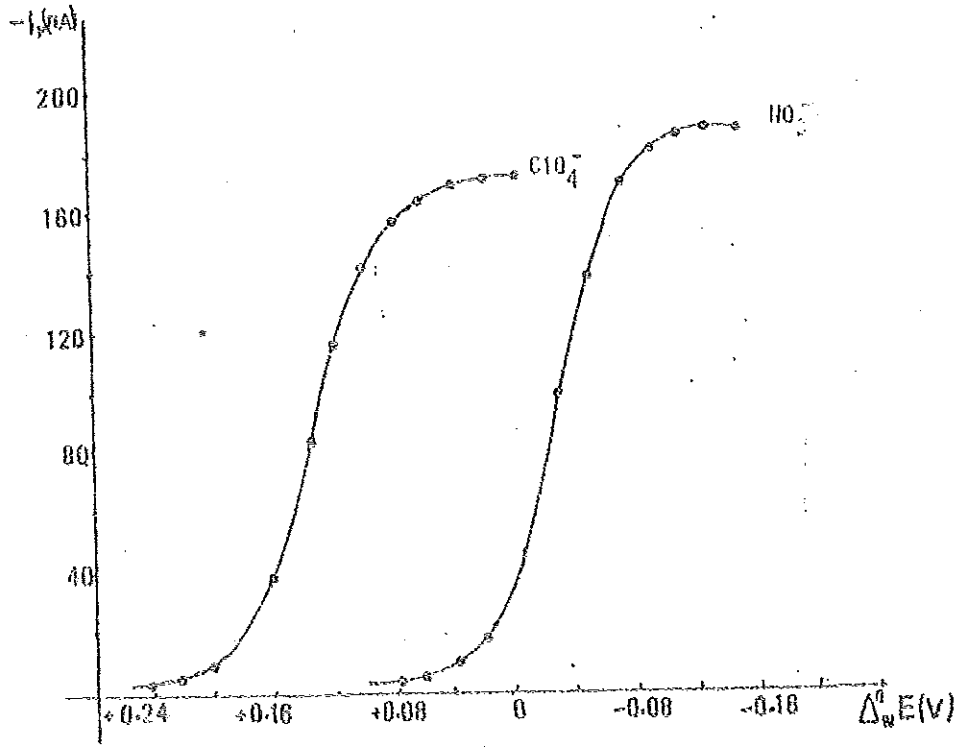

Fig. 17. Dependence of the peak height on the applied potential difference for 0.1 mM ClO_4^- and 0.1 mM NO_3^- supporting electrolyte in the aqueous phase 100 mM $Mg SO_4$ and in the organic phase 10mM CVTPB.

Table 3 Dependence of peak current (ip) on the applied potential and concentraion for ClO_4^-. (Potential in volt (V) concentration in millimolar (mM) and current in nanoampere (nA))

$\Delta_W^o E$(V)	1 mM	0.5 mM	0.1 mM	.05 mM	.01 mM	.005 mM	.001 mM
+.200	82	38	8	4	-	-	-
+.160	495	250	51	26	5	3.0	-
+.140	805	430	84	42	8	4.5	2.8
+.120	1095	550	115	57	12	6.0	3.0
+.100	1385	710	143	72	14	7.5	3.5
+.080	1490	785	158	79	16	8.0	4.0
+.060	1540	805	170	85	17	8.6	4.0
+.025	1630	855	172	86	17	8.6	4.0
-.030	1640	855	172	86	17	8.6	4.0

Table 4 Dependence of peak current (ip) on the applied potential and concentration for NO_3^- (Potential in volt (V) concentration in millimolar (mM) and current in nanoampere (nA)).

$\Delta_W^O E$(V)	1 mM	0.5 mM	0.1 mM	0.05 mM	0.01 mM	.005mM	.001mM
+.040	50	36	6	4	-	-	-
+.060	75	36	8	4	3	-	-
+.025	168	90	18	9	3	-	-
+.030	920	505	100	51	10	6	3.0
+.050	1360	702	141	72	14	8	3.5
+.070	1640	850	170	86	17	9	3.6
-.090	1710	910	182	91	18	9	4.1
-.110	1720	935	187	94	19	9	4.2
-.120	1730	935	187	94	19	9	4.2

Table 5 Dependence of peak current (ip) on the applied potential and concentration for Cl^-.(Potential in volt(V),concentration in millimolar(mM) and current in nanoamperes(nA)).

$\Delta_W^O E$(V)	1mM	0.5mM	0.1mM	0.05mM	0.01mM	0.005mM
-.050	92	46	10	7	-	-
-.070	145	74	16	8	-	-
-.090	195	115	22	12	3	3 0
-.110	310	172	34	17	4	3.5
-.120	398	216	42	22	5	3.5
-.140	602	324	65	33	7	4.0
-.160	895	478	96	48	10	6.0

depend on the nature of the ion to be transferred across ITIES. The half wave Galvani potential difference is closely related to the standard Galvani potential difference. $\Delta^{o}_{w}\varphi^{o}_{i}$ Both of them can be used for qualitative determination of the substance. For two ions the difference in the standard Galvani potential difference is constant. Based on this fact the difference between;

$$\Delta^{o}_{w}\varphi_{1/2NO^{-}_{3}} - \Delta_{w}\varphi_{1/2ClO^{-}_{4}} = \Delta_{w}E_{1/2NO^{-}_{3}} - \Delta_{w}E_{1/2ClO^{-}_{4}} \qquad 31$$

was calculated. The value obtained based on this calculation is -0.170V which is in a good agreement with those reported in Ref. 9 and 35, namely - 0.163V and - 0.171V respectively

4.2. Quantitative Determination of Perchlorate and Nitrate

The application of the detector for the quantitative determination of anions is shown in Fig 18 for ClO^{-}_{4} and NO^{-}_{3} In both cases a linear relationship between the limiting current (i_l) and the concentration of the analyte was obtained. But a slight deviation from linearity was observed for concentrations higher than 0.5 mM and lower than 0.001 mM. This limiting current usually depends on the amount of ion transferred across the ITIES. The ion transfer process was found to be diffusion controlled.

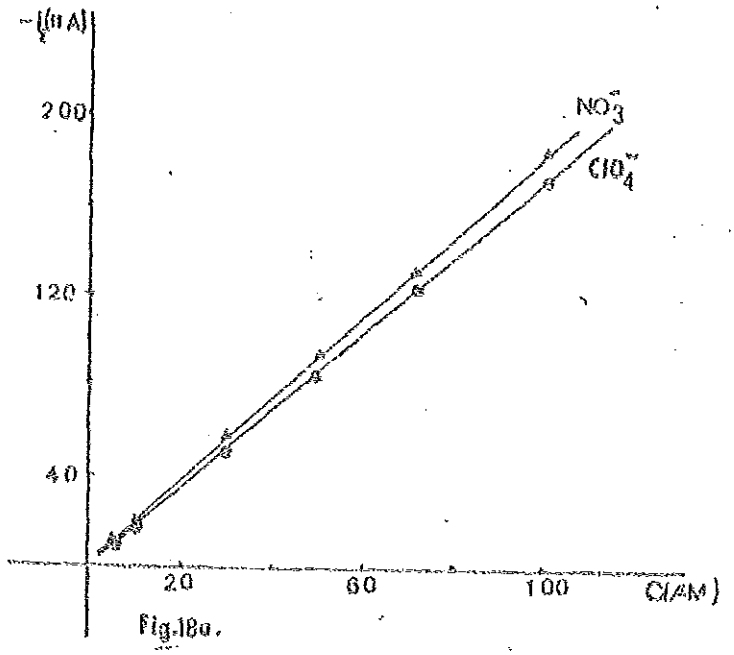

Fig.18a.

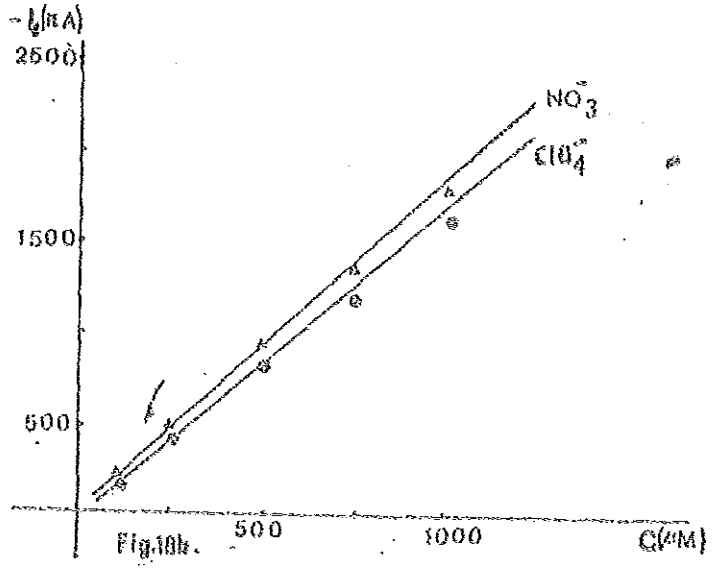

Fig.18b.

Fig.18a and 18b. Dependence of peak height on the concentration of 0.1 mM of ClO_4^- and 0.1 mM of NO_3^- in the sample injected Fig 18a for lower concentration and Fig 18b for higher concentration.

4.3. Determination of Sodium and Potassium by facilitated ion transfer with Dibenzo-18-Crown-6.

Dibenzo-18-crown-6 (DB-18-C-6) is an aromatic cyclic polyether (Fig 19) which can form a stable complex

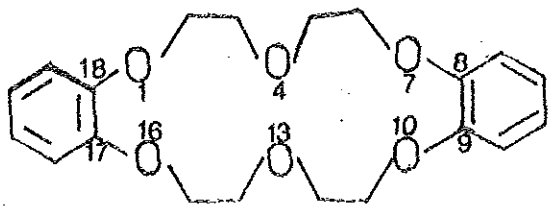

Fig. 19 Dibenzo-18-crown-6

with Na^+ and K^+. This complex is formed by ion dipole interaction between the cation and the oxygen atoms symmetrically placed in the polyether ring.

The transfer of K^+ and Na^+ across the ITIES can be facilitated through complexation with this ligand (69 & 45). Fig 20 and 21 and also Tables 6 and 7 demonstrate the effect of the neutral synthetic ligand on the transfer of the monovalent cations K^+ and Na^+ across the water/nitrobenzene interface. The positive peak current similar to Fig 15 obtained during the measurement can be ascribed to the transfer of the metal ion from water to nitrobenzene induced by the complex formation at the interface. Values of the positive peak currents obtained at different potentials and different concentrations for K^+ and Na^+ are summarized in tables 6 and 7.

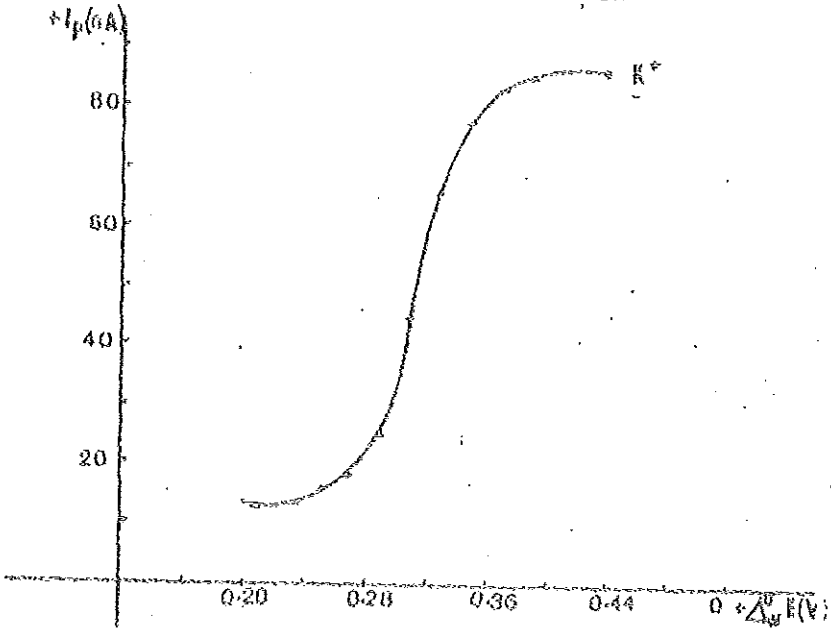

Fig. 20. Dependence of the peak height on the applied potential difference for K^+ in the absence of DB-18-C-6

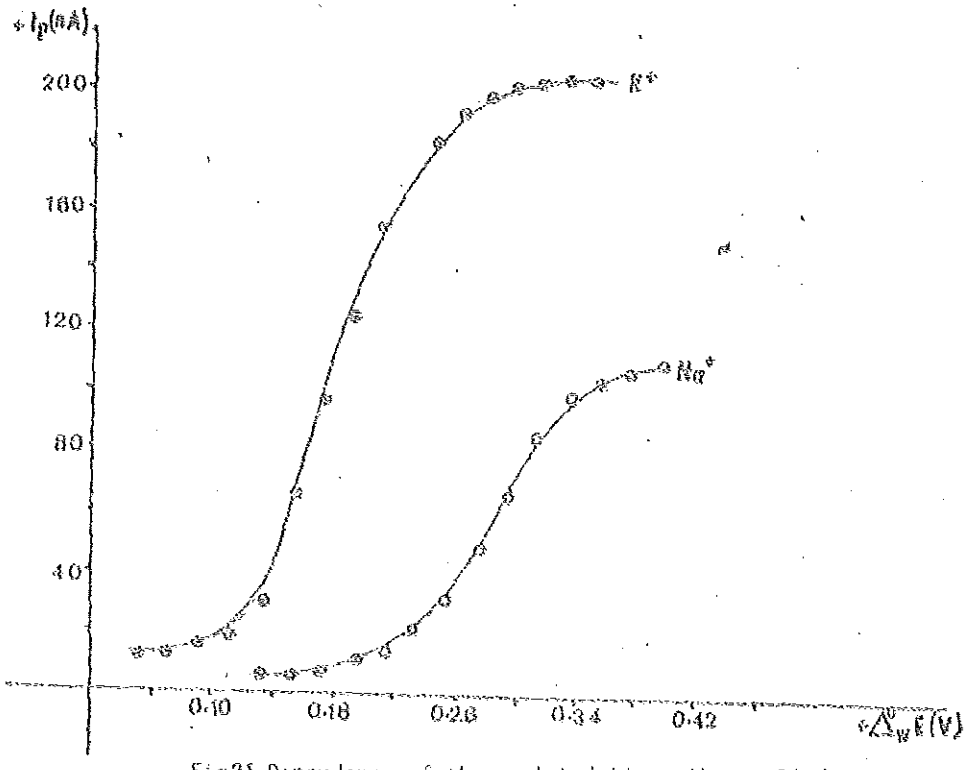

Fig21. Dependence of the peak height on the applied potential difference for Na^+ and K^+ in the presence of neutral carrier (DB-18-C-6)

Table 6a Dependence of peak current (ip) on the applied potential and concentration for K^+ in the abesence of DB-18-C-6.(Potential in volt (V) concentration in millimolar (mM) and current in nanoampere (nA)).

$\Delta^o_w E$(V)	1 mM	0.5 mM	0.1 mM	0.05 mM	0.01 mM	0.005 mM
.206	120	48	13	3	3.0	-
.227	162	62	17	10	5.0	-
.246	173	82	18	12	6.0	2.8
.265	198	155	20	12	7.0	3.0
.286	246	215	25	12	7.5	3.5
.306	453	265	46	23	8.0	3.8
.326	648	330	66	34	8.2	4.2
.346	682	380	69	39	8.2	4.5
.366	818	430	83	42	9.0	4.8
.386	834	470	85	45	9.2	5.1
.405	840	480	85	45	9.2	5.2
.426	846	480	86	45	9.2	5.2

Table 6b Dependence of peak current (ip) on the applied potential and concentration for K^+ in the presence of DB-18-C-6.(Potential in volt (V) concentration in millimolar (mM) and current in nanoampere (nA)).

$\Delta^{O}_{W}E$(V)	1mM	0.5mM	0.1mM	0.05mM	0.01mM	0.005mM	0.001mM
.087	155	71	15	8	-	-	-
.108	198	138	20	10	-	-	-
.130	240	255	25	13	6	-	-
.149	610	300	63	31	7	-	-
.168	950	445	96	45	10	6	2.5
.187	1010	620	126	63	13	7	3.0
.206	1480	778	154	78	15	8	3.0
.226	1610	820	166	83	17	9	3.2
.245	1790	910	185	93	19	10	3.4
.264	1880	950	194	96	20	10	3.5
.286	1910	1000	200	100	20	11	3.6
.307	1950	1020	202	102	21	11	3.8
.327	1960	1020	204	102	21	11	4.5
.347	1960	1020	204	102	21	11	5.0

Table 7 Dependence of peak current (ip) on the applied potential and concentration for Na^+ in presence of DB-18-C-6.(Potential in volt (V) concentration in millimolar (mM) and current in nanoammpere (nA)).

$\Delta_W^O E$(V)	1 mM	0. 5mM	0.1 mM	0.05 mM	0.01 mM
.130	64	18	6	-	-
.150	74	21	7	-	-
.168	81	38	8	-	-
.187	128	56	13	7	-
.206	178	82	18	9	-
.225	241	120	25	13	-
.244	362	175	37	19	5.0
.264	471	245	48	25	7.0
.386	665	325	68	36	10.0
.306	807	410	88	44	12.0
.327	995	480	102	54	12.1
.346	1005	510	105	56	12.2
.366	1010	530	108	58	12.2
.386	1030	540	110	58	12.2
.406	1030	540	110	58	12.4

The quantitative determination of K^+ is shown in Fig 22. As one can see from the graph the limiting current is directly proportional to the concentration of the injected hydrophilic cation. The concentration of DB-18-C-6 in the nitrobenzene was 10mM which was much greater than the concentration of K^+ or Na^+ in the aqueous phase. This indicates that the limiting current (i_l) is controlled by the diffusion of K^+ or Na^+ from the bulk aqueous to the membrane stabilized interface.

Fig 20 and 21 or Tables 6a and 6b show the current - potential dependence for tne transfer of K^+ through the interface in the absence and presence of the electro neutral carrier DB-18-C-6 in the nitrobenzene phase. As one can see from the diagram the transfer of K^+ in the presence of neutral carrier starts at a more negative potential than the transfer of K^+ in the absence of neutral carrier. This is because the transfer of K^+ in the presence of neutral carrier is facilitated through complex formation with this ligand. Because of this the limiting current obtained for K^+ in facilitated system will not be influenced by the transfer of the supporting electrolytes (Mg^{+2} or TPB^-). As a result a higher limiting current is obtained as shown in Fig 21. For Na^+ in the absence of neutral carrier a voltamogram similar to Fig 20 was not obtained since the transfer of TPB^- from the nitrobenzene and Mg^{+2} from the aqueous phase interfere with the transfer of Na^+ from water to nitrobenzene. As one can see from Table 8

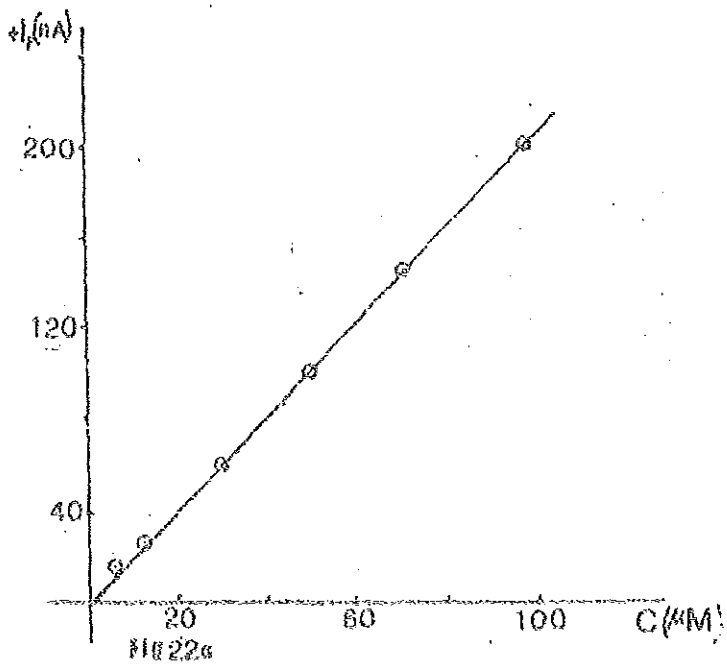

Fig 22a

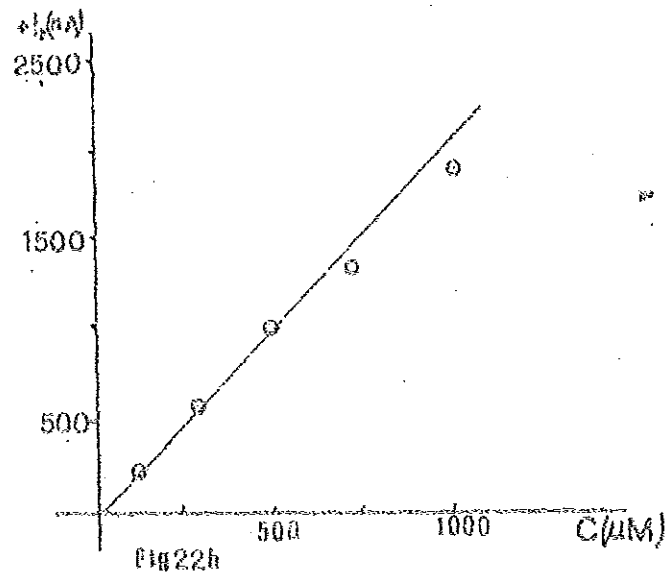

Fig 22b

Fig 22a &b Dependence of peak height on the concentration of H^+ in the presence of neutral carrier Fig 22a for lower concentration and Fig 22b for higher concentration.

Table 8 Values of standard Galvani-potential difference

Ions	$\Delta_o^{\omega} \varphi_i^{\circ}$ (V)
Mg^{+2}	.370
TPB^{-}	.372
Na^{+}	.358
K^{+}	.252

the value of the standard Galvani potential difference of Na^{+} is very close to TPB^{-} and Mg^{+2} while in the case of K^{+} there is a difference of.118V between the value of Mg^{+2} and TPB^{-}.The transfer of K^{+}may therefore be possible without the interference of Mg^{+2} and TPB^{-}.

4.4. Application to artificial standard and blood serum samples

Sodium is the major cation of extracellular fluid. As a result all the blood sodium is found in the serum. The normal range of sodium levels in serum is about 130 - 150 mM while potassium is the major intracellular cation, having an average cellular concentration of 105 mM in red cells (92). The normal range of potassium levels in serum is about 3.5 to 5 mM which is about 0.04 times lower than the concentration of potassium in intracellular fluid.

Low serum sodium level(Hyponatremia) and increased serum sodium level (Hypernatermia) as well as low serum potassium levels (Hypokalemia) and increased serum potassium level (Hyperkalemia) can cause various diseases (see Ref 92 and 93). For example, levels of potassium around 10 mM may be fatal. For these reasons the serum sodium and serum potassium determination have become a most important diagnostic tool in situations in which extremely high or low serum potassium levels are suspected.

Although a number of gravimetric and titrimetric methods for the determination of sodium and potassium in body fluids are available, these are outdated, slow and require large amounts of specimen. Almost all laboratories today employ either emission flame photometry or atomic absorption spectrophotometry for this test because of the speed and simplicity of these method. A new and promising approach to the determination of sodium and potassium in body fluids makes use of ion selective electrodes, an extension to this method for the determination of these cations have been proposed using the transfer of these cations across the membrane stabilized ITIES.

Specimens for serum potassium analysis must be free from hemolysis, since any release of potassium from red cells can significantly increase the serum levels and thus invalidate the test results. In addition to this if the

serum is not separated from the blood shortly after collection of the blood, there is some movement of potassium ions out of the cells (a shift of potassium from the cell to the serum) which can cause an increase in potassium level of the serum. Therefore in order to overcome this problem the serum should be separated from the blood shortly after collection of the blood.

For this experiment the serum was separated from the blood immediately after collection of the blood and diluted to a ratio of 1:50 i.e. 0.5 ml of the serum was diluted with 45 ml of redistilled water. Before the serum and the artificial samples (a mixture of Na^+ and K^+ of different concentration) were analyzed for their Na^+ and K^+ concentration a series of standard solution of K^+ and Na^+ were prepared. Fig 23a shows the absorbance of K^+ at wave length 767 nanometrer(nm) and Na^+ at a wave length 589 nanometer (nm) in flame analyzer and Fig 23 b c d & e the peak current value of these cations obtained in voltammetric sensor at two different potentials for a series of standard solution of these cations. In both cases linear calibration graphs as shown in Fig 23 were obtained.

The analytical results obtained by a voltammetric sensor, along with those obtained by the flame photometry methods are summarized in Tables 9,10, and 11. Table 9 indicates the absorbance of potassium at a wave length of 767

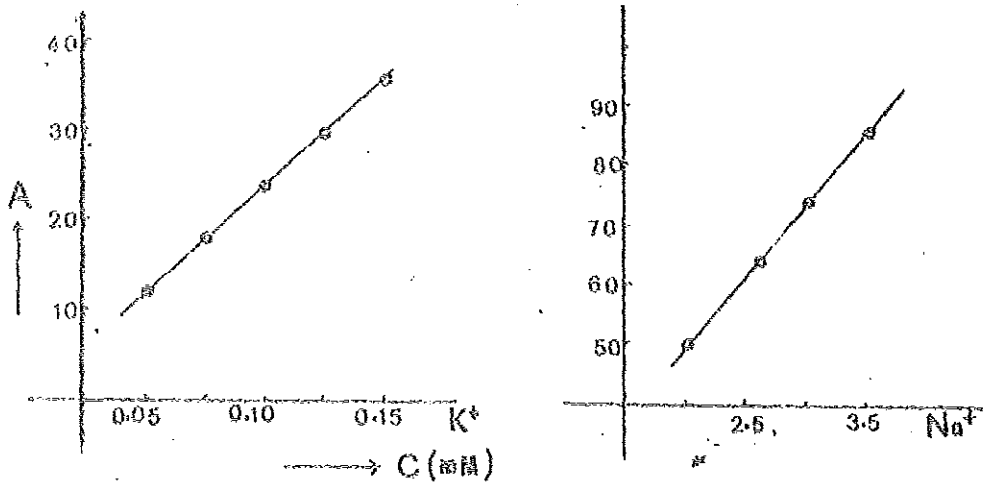

Fig 23a A calibration graph for absorbance of Na^+ at 589 n.m and K^+ at 767 n.m in flame analyzer

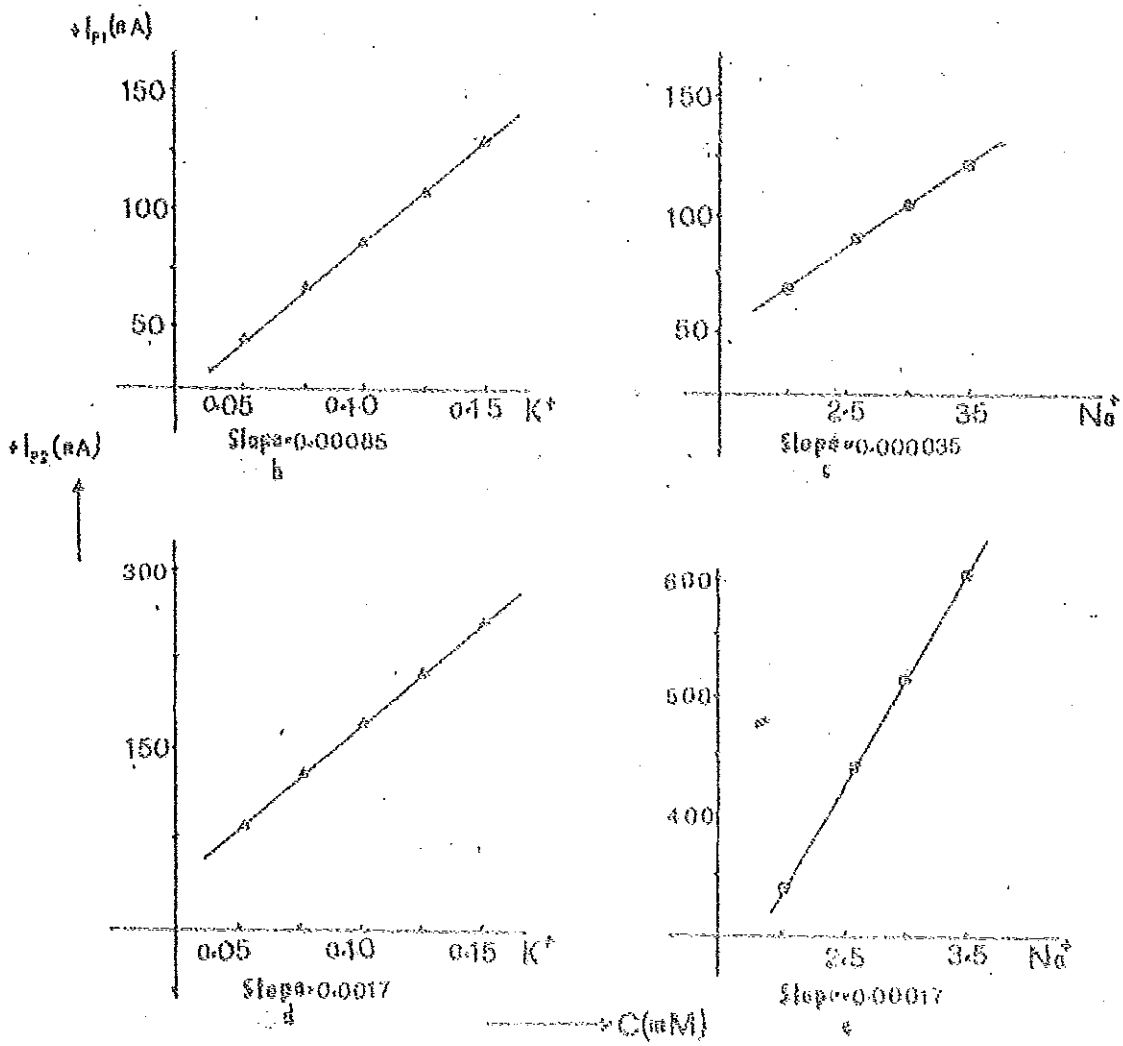

Fig.23b,c,d,e. Calibration graphs for peak currents (ip_1 at 170mV and ip_2 at 238mV) for standard samples of K^+ and Na^+. From the slope of the graph the partial sensitivity (b1) can be determined.

Table 9 Peak current and absorbance for aritificial and blood serum samples. Current in nanoampere (nA) and Wave length in nanometer (nm)

Samples No.	+ip (nA) at 170 mV	+ip (nA) at 238 mV	absorbance at 767 nm K	absorbance at 589 nm Na
1	147	590	12	73
2	150	510	24	50
3	189	674	24	74
4	195	595	35	50
5	205	645	33	59
6	187	650	26	69
7	165	610	20	72
8	160	595	18	70
9	180	650	24	69
10	185	660	23	70
11	155	580	16	70
12	158	600	17	69

N.B No 1-6 artificail samples and from No 6-12 blood serum samples

Table 10 Concentration of K^+ and Na^+ in artificial samples (mixtures of Na^+ and K^+) by voltammetric sensor and flame analyser.(Concentration in millimolar(mM))

Sample No.	Certified Concentration (mM)		Concentration found voltammetric sensor (mM)		Concentration found flame analyser (mM)	
	K^+	Na^+	K^+	Na^+	K	Na
1	0.05	3.00	0.05	2.96	0.05	2.98
2	0.10	2.00	0.90	2.10	0.10	2.00
3	0.10	3.00	0.10	2.96	0.10	3.00
4	0.15	2.00	0.15	2.05	0.15	2.00
5	0.14	2.26	0.14	2.35	0.14	2.40
6	0.11	2.72	0.11	2.76	0.11	2.80

Artificial samples were obtained from Boehringer Manheim company for control sera (after 1:50 dilution of the sample the recommended accepted range is 0.127mM - 0.15mM for K^+ and 2.12mM - 2.4mM for Na ,the value given for No.5 and 6 is the average value.)

Table 11a. Concentrations of K^+ and Na^+ in blood serum sample after 1:50 dilution in voltammetric sensor and flame analyser.(Concentration in millimolar (mM)).

sample No.	Voltammetric sensor		Flame analyser	
	K^+	Na^+	K	Na
7	0.079	2.80	0.083	2.92
8	0.075	2.75	0.075	2.84
9	0.092	2.90	0.100	2.80
10	0.098	2.90	0.096	2.84
11	0.071	2.70	0.069	2.84
12	0.069	2.84	0.071	2.80

Table 11b. Determined values of K^+ and Na^+ in artificial and blood serum samples using voltammetric sensor and flame analyser when the result shown in table 11 a are multiplied by 50.Concentration in millimolars (mM)

Sample No.	Voltammetric sensor		Flame analyser	
	K^+	Na^+	K	Na
5	7.0	117.5	7.00	120
6	5.3	138.0	5.40	140
7	3.95	140.0	4.15	146
8	3.75	137.5	3.75	142
9	4.6	145.0	5.00	140
10	4.9	145.0	4.80	142
11	3.55	135.0	3.45	142
12	3.45	132.0	3.55	140

Standared samples prepared by Boehringer Mannheim for controls sera

No.5 : $[K^+]$av = 6.92 mM accepted range 6.37 - 7.43 mM

$[Na^+]$av = 113 mM accepted range 106 - 120 mM

No.6 : $[K^+]$av = 5.28mM accepted range 4.86 - 5.70 mM

$[Na^+]$av = 136mM accepted range 128 - 144 mM

Sample Nos.7-12 are blood serum samples Normal range of Na^+ in blood serum :130-150mM Normal range of K^+ in blood serum :3.5-5.6mM

nm and sodium at a wave length 589 nm in flame analyzer and the peak current values of these cations in voltammetric sensor for the artificial prepared samples and blood serum samples. As one can see from table 10 and 11 the values obtained by the two methods are in a good agreement with each other as well as with the values for the control sera samples (samples No 5 & 6) given by Boehringer Mannheim. All are in the range of the normal levels of sodium and potassium in blood serum (see Table 11b)

When the voltammetric sensor is used for the determination of Na^+ and K^+ in the mixture of the two cations the interference of sodium in the determination of potassium and vice versa was observed. Because of this to determine the concentration of each cation in the sample solutions the assumption given in section 4.5.1 specifically equation 34 was used (see the details in section 4.5.1). Based on this assumption the values of the partial sensitivity of the cations at two different potential was determined from the slope of the graphs shown in Fig 23b,c,d and f.

The equation used for the determination of K^+ and Na^+ in the artificial and blood samples by using a voltammetric

sensor is given by

$b_1 [k^+] + b_2[Na^+] = ip_1$ at ΔE_1
$b_1' [k^+] + b_2'[Na^+] = ip_2$ at ΔE_2

which is based on equation 34 section 5.1 where ip_1 and ip_2 the peak currents obtained at ΔE_1 and ΔE_2, b_1 and b_1' is the partial sensitivity of K^+, b_2 and b_2' the partial sensitivity of Na^+ at ΔE_1 and ΔE_2 respectively. The values obtained from the slope of the graph Fig 23b,c,d and e,which are the partial sensitivities are given below

$b_1 = 0.00085$ $b_2 = 0.000035$

$b_1' = 0.00170$ $b_2' = 0.00017$

Substituting these values in the above equation we can get
$0.00085[K^+] + 0.000035[Na^+] = ip_1$ at 170 mV
$0.00170[K^+] + 0.00017[Na^+] = ip_2$ at 238 mV
if the values in Table 9 are substituted for ip_1 and ip_2 the concentration of K^+ and Na^+ can be determined. Table 11 and 12 are compiled based on this calculations.

If one wants to determine the potassium level in the absence of sodium, it may be possible to use the blood red cell sample instead of the blood serum.

4.5. Selectivity

When the detector is applied for the determination of an ion A in the presence of interfering ions B, C...I, each ion will contribute to the current ip, taken as the signal proportional to the concentration. Thus one can write (69).

$$ip = \kappa \Sigma b_i c_i \qquad 32$$

where b_i is the partial sensitivity of the i ion in the sample and $\kappa = 1.38nF\upsilon^{-5/12} \alpha^{-1/2} R^{3/4} V^{3/4}$ 33

The value of b_i for a particular ion is potential dependent and it is constant at the limiting current potential of the ion.

In order to evaluate the influence of the partial sensitivity of the method, the effect of NO_3^- and Cl^- on the determination of ClO_4^-, the effect of ClO_4^- and Cl^- on the determination of NO_3^- and the effect of Na^+ on the determination of K^+ have been investigated. These investigations were made by preparing a mixture of these anions and cations as shown in Tables 12 13 and 14. As one can see from this table the interference of Cl^- in the determination of ClO_4^- is negligible. It is possible to determine 0.01 mM of ClO_4^- in the presence of 1mM of Cl^- with out the interference of Cl^-. This can be taken as the tolerance limit (permissible level) of Cl^- in the

Table 12. Selectivity studies on ClO_4^-. Concentration in millimolar (mM), current in nanoampere (nA)

* 1	2	3	4	5	6	7	8	9
0.100	143	14.5	-	4	-	145	28	160
0.080	158	16.0	-	21	3.0	160	32	170
0.060	162	16.4	-	50	6.0	165	65	210
0.040	170	17.3	6	75	8.4	176	81.	240
0.025	172	17.4	12	168	18.4	180	185	340
-0.030	172	17.4	20	920	100.0	268	935	1085

*

1 = $\Delta_W^O E$(V) 2 = 0.1 ClO_4^- mM 3 = 0.01 ClO_4^- mM

4 = 1.0 Cl^- mM 5 = 1.0 NO_3^- mM 6 = 0.1 NO_3^- mM

7 = 0.1 mM ClO_4^- + 1.0 mM Cl^- + 0.1 mM NO_3^-

8 = 0.01 mM ClO_4^- + 1.0 mM Cl^- + 1.0 mM NO_3^-

9 = 0.1 mM ClO_4^- + 1.0 mM Cl^- + 1.0 mM NO_3^-

Table 13. Selectivity studies on NO_3^- concentration in millimolar (mM),current in nanoampere(nA)

* 1	2	3	4	5	6	7	8	9
0.03	100	51	-	172	1640	1780	1680	186
0.05	141	72	92	172	1645	1840	1750	192
0.07	170	86	145	172	1650	1890	1780	203
0.09	182	91	195	171	1640	1950	1810	208
0.11	187	94	310	171	1640	2030	1900	220
0.12	187	94	398	171	1630	2120	2070	226

* 1 = $\Delta^{O}_{W}E$(V) 2 = 0.1 NO_3^- mM 3 = 0.01 NO_3^- mM

4 = 1.0 Cl^- mM 5 = 0.1 ClO_4^- mM 6 = 1.0 ClO_4^- mM

7 = 0.10 mM NO_3^- + 1.0 mM Cl^- + 1.0 mM ClO_4^-

8 = 0.01 mM NO_3^- + 1.0 mM Cl^- + 1.0 mM ClO_4^-

9 = 0.01 mM NO_3^- + 0.1 mM Cl^- + 0.1 mM ClO_4^-

Table 14. selectivity studies on K^+ concentration in millimolar (mM), current in nanoampere (nA)

* 1	2	3	4	5	6	7	8	9
0.175	92.0	9.5	30.0	4.0	93	120	12	40
0.188	110.0	11.2	51.0	5.2	113	160	15	52
0.200	145.0	14.8	90.0	9.2	153	232	22	100
0.220	160.0	16.0	135.0	13.6	170	289	28	148
0.240	175.0	17.6	178.0	18.0	188	356	34	182
0.250	185.0	18.7	240.0	24.0	205	420	41	254
0.270	200.0	20.2	340.0	34.2	228	535	53	362
0.290	205.0	20.6	467.0	47.0	240	675	65	478
0.310	210.0	21.3	600.0	60.0	256	805	79	613
0.330	210.0	21.2	700.0	70.2	275	895	80	718

* 1 = $\Delta^{O}_{W}E(V)$ 2 = 0.1 K^+ mM 3 = 0.01 K^+ mM

4 = 1.0 Na^+ mM 5 = 0.1 Na^+ mM

6 = 0.1 mM Na^+ + 0.1 mM K^+

7 = 1.0 mM Na^+ + 0.1 mM K^+

8 = 0.1 mM Na^+ + 0.1 mM K^+

9 = 1.0 mM Na^+ + 0.1 mM K^+

determination of ClO_4^- . While the interference of NO_3^- on the determination of ClO_4^- is considerable even at equal concentration of both anions. In the determination of NO_3^- the interference of ClO_4^- is very high even at its lowest concentration. This is because the transfer of ClO_4^- across the interface starts before NO_3^- . Though the transfer of Cl^- ion will start after NO_3^- there is a considerable interference of Cl^- in the determination of NO_3^- even at equal concentration of both anions. A similar situation was also observed for K^+ and Na^+ cations (table 14) . This can be taken as one of the draw backs of the detector.

However if the concentration of the interfering ions can be determined by other methods, the signal can easily be corrected. In addition to this if the partial sensitivity of the two ions are determined at two different potential one can have a simultaneous equation based on equation 32.

$$ip_1 = b_1 c_A + b_2 c_B \quad \text{at } \Delta E_1$$
$$ip_2 = b'_1 c_A + b'_2 c_B \quad \text{at } \Delta E_2 \qquad 34$$

where ip_1 and ip_2 are the peak currents at ΔE_1 and ΔE_2 , b_1 and b'_1 the partial sensitivity of the ion c_A , b_2 and b'_2 the partial sensitivity of the ion c_B at a potential ΔE_1 and ΔE_2 respectively. Since the partial sensitivity (b_i) of a particular ion is constant at the limiting current potential of the ion, at least one of the equation should not be at this region. The value of b_i for a particular ion can be

determined from the linear calibration graph of current vs concentration of the ion at a given potential. The slope of this graph is equal to the partial sensitivity (b_i) of the ion, so that if the values of b_i are calculated, based on equation 34, the value of c_A and c_B can be determined.

4.6 Precision:-

In order to investigate the reproducibility of the method, 13 peak currents were run for the determination of the same concentration of perchlorate. The same type of measurements were also taken for five different concentration of perchlorate(0.1, 0.08, 0.06 0.04 and 0.02 mM of ClO_4^-). The peak currents obtained are shown in Fig 24. Table 15 indicates the mean and standard deviation of these peaks. These observations depict that the method developed gives reproducible results.

However the limiting or the peak current can be varied if the relative position and the relative distance between the membrane stabilized and the tip of the nozzle is changed. These changes can have an effect on the flow rate parameter (α) and the radius of the electrode surface (R) where

$$i_l = \text{constant } V^{\alpha} R \qquad 35$$

One of the factor which can determine the value of α is the relative distance between the tip of the nozzle and the electrode surface (interface)(94) and it is maximum equal to

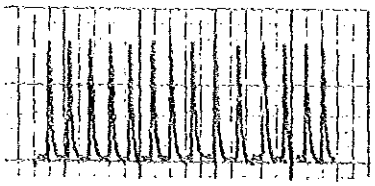

Conc.0.02 mM
Sensitivity 5mV

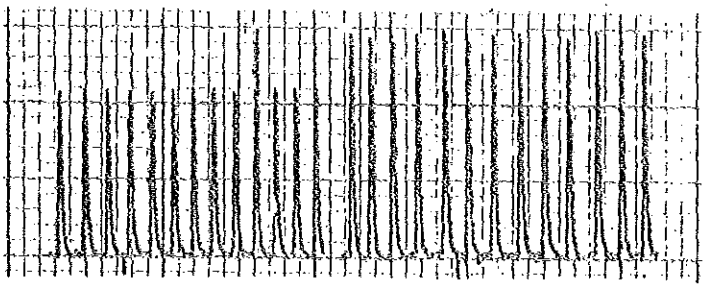

Conc. 0.06 mM
Sensitivity 10mV

Conc 0.04 mM
Sensitivity 5mV

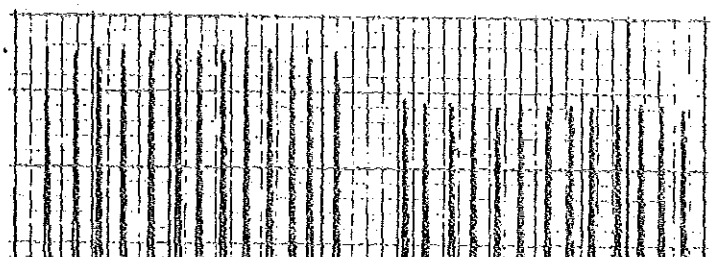

Conc. 0.1 mM
Sensitivity 10mV

Conc. 0.08 mM
Sensitivity 10 mV

Fig.24. The peak currents for 5 standard samples of ClO_2^- and 13 measured peak currents of each samples

Table 15. The peak current (ip) obtained for 5 standard sample of ClO_4^- and for 13 measurements of each samples.(Concentration in millimolar(mM), current in nanoampere(nA)).

No. of measurements	0.1 mM	0.08 mM	0.06 mM	0.04 mM	0.02 mM
1	177.5	144.0	107.3	73.0	37.9
2	175.5	142.4	108.5	72.0	37.9
3	177.1	142.4	108.5	73.0	38.3
4	176.7	142.0	108.5	73.0	38.3
5	177.5	142.0	108.5	73.0	38.7
6	176.7	142.0	108.5	73.0	37.9
7	177.5	142.0	109.7	73.0	37.9
8	178.3	142.0	109.7	73.0	37.5
9	178.3	142.0	109.7	73.0	37.5
10	177.5	142.0	108.5	72.0	37.5
11	175.5	142.0	109.7	73.2	37.5
12	174.4	142.0	108.5	73.0	37.5
13	175.5	140.0	108.5	73.0	37.5
mean	176.77	142.08	108.59	72.86	37.84
S.D.	1.2037	0.8357	0.6588	0.3863	0.3948

S.D = standard deviation

0.75 for a wall jet cell arrangement.The impinging jet of solution should fall at the centre of the surface of the electrode (ITIES). If these parameters are not kept constant the reproducibility of the detector can be changed. To overcome this problem a wall jet cell shown in Fig 25 is recommended. As shown in the diagram the reference electrode for the aqueous phase, the compartment of the organic phase (to which the membrane stabilized interface is attached), the nozzle (jet inlet and counter electrode for the aqueous phase) and the outlet can be so fixed that one can have a fixed relative distance and position between the interface and the tip of the nozzle. Through the hole indicated by number 5 in the diagram a thin plastic covered wire of the type shown by No.4 can be inserted and bubbles can be removed if they are formed during the measurement. By the help of the fixed outlet the level of the supporting electrolyte in the cell can be kept constant. The cell is graduated in order to check the flow rate during the measurement time.

Another factor which can influence the reproducibility of a detector is the condition of the porous membrane. The porous membrane may be blocked by the precipitates formed if it is used for more than three weeks.

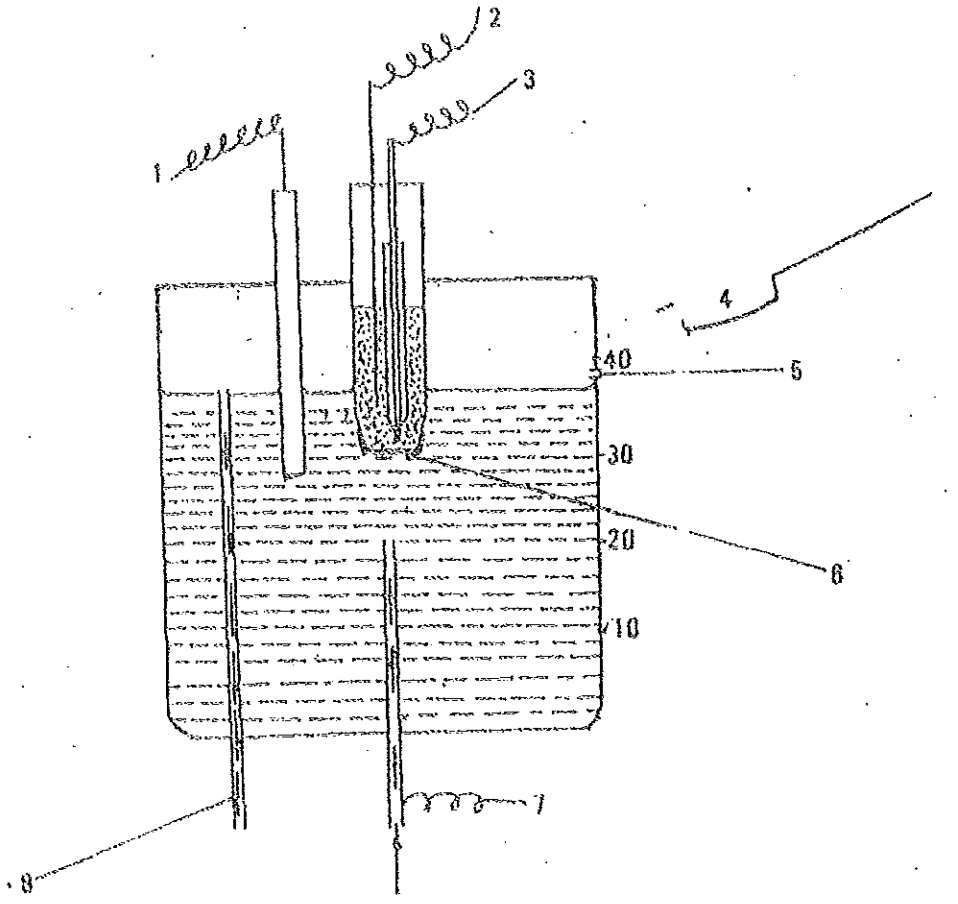

Fig.25. Graduated wall jet cell which is covered at the top and bottom and all the components are fixed at the covers. (1) and (3) Reference electrodes, (2) counter electrode in the organic phase, (4) plastic covered wire which is desigened to remove the bubbles at the membrane surface, (5) an inlet for the plastic covered wire, (6) membrane , (7) jet inlet (stainless steel needle) serves as counter electrode, (8) outlet.

4.7 Detection limit

The detection limit of an analytical system as recommended by the Analytical Methods Committee(95), can be defined as the concentration (c_L)or amount (q_L) corresponding to a measurement level $3\sigma_B$ units above the value of zero analyte. Where $3\sigma_B$ is the standard deviation of the responses of the field blanks. The value of σ_B obtained for the peaks of redistilled water (zero analyte concentration) was 0.833.

$$3\sigma_B = 3(0.833) \qquad 36$$
$$= 2.5$$

This value corresponds to 0.25 μM ClO_4^- (Fig. 26), which is the detection limit of the method obtaind for perchlorate ion.

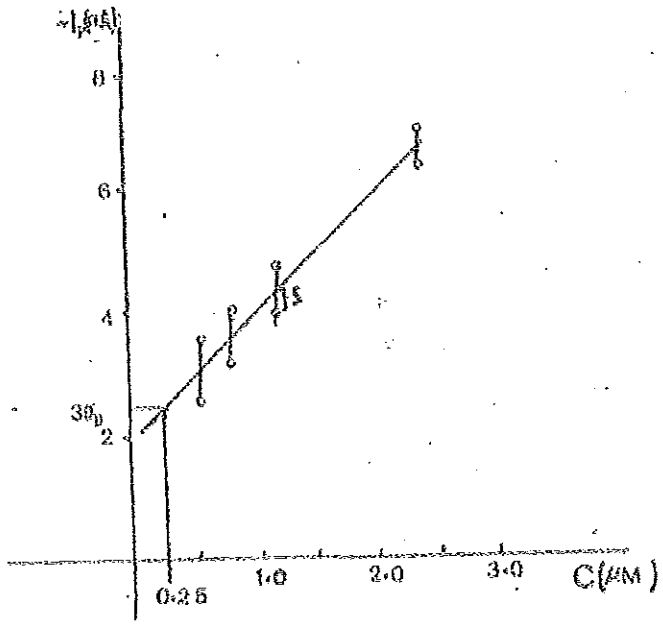

Fig.26. Dependence of the peak height on the concentration of ClO_4^- in the sample injected at low concentrations. The vertical bars show the standard deviations obtained from 11 runs for each concentration.

5 Conclusion

The analytical application of the voltammetric sensor which is constructed in our laboratory is based on the transfer of anions and cations across the membrane stabilized interface of two immiscible electrolyte solutions in a flow injection system. Hydrophilic cations like sodium and potassium have been determined in the presence of neutral carrier in the organic phase. The iR drop resulting from the dilution effect of the distiled water at the interface has been compensated by increasing the concentration of the supporting electrolyte in the aqueous phase. Qualitative determination of the ions have been made based on the half- wave Galvani potential difference of the S-shaped polarographic curves and quantitative determinations were based on the limiting current values. The effect of interfering ions can be corrected if the concentration of the ion is determined by other methods or if the partial sensitivity of the ion is determined at two different applied potentials. The method has been tested by applying it to the determination of sodium and potassium in blood serum samples in the presence of a neutral carrier and the results obtained by the method are in a good agreement with the flame photometric method.

The results obtained from the various studies and statistical evaluation of the method indicates that the proposed method is sensitive, rapid, simple, reliable, reproducible and requires small amount of specimen. Therefore the method can be used for the determination of some anions and cations in various samples

6.REFERENCES

1. J.Koryta, *Electrochim .Acta.*, 24 (1979) 293.
2. J.Koryta, *Electrochim.Acta.*, 33 (1988) 189.
3. J.Guastala, *J.Chim.phy.*,53 (1956) 474.
   C.Gavach,T.Mlodnicka and J.Guastalla, *C.r.Acad.Sci,Ser*, C266 (1968) 1196 *Chem.Abstr.*, 69 (1968) 7815C
5. M. Blank, *J. colloid Interface Sci*, 22 (1966) 51 *Chem Abstr.*, 65 (1966) 97736
6. P. Joos and M. Van Bockstaele, *J. phys. Chem.*, 80 (1976) 1573.
7. P. Joos, *J. Electroanal. Chem.*, 84 (1978) 75
8. J. Koryta, P. Vanysek and M. Brezina, *J. Electroanal. Chem.*, 75 (1977) 211
9. J. Koryta, *Electrochim.Acta.*, 29 (1984) 445
10. H.H. Girault, *Electrochim. Acta.*, 32 (1987) 445
11. S.Kihara, M. Suzuki, K. Maeda, K. Ogura, S.Umetani, M. Matsui and Z.Yoshida, *Anal. Chem.*, 58 (1986) 2954.
12. J.Koryta, *Anal. Chem. Acta.*, 159 (1984) 1.
13. J.Koryta, *Anal. Chem. Acta.*, 183 (1986) 1.
14. J.Koryta, *Electrochim. Acta.*, 31 (1986) 516.
15. J.Koryta, *Electrochim Acta.*, 32 (1987) 419.
16. P. Vanysek and R.P. Buck, *J. Electroanal. Chem.*, 173 (1984) 1.
17. P. Vanysek and F. Henry, *J. Electroanal.*,*Chem.* 179 (1984) 131.
18. C.Gavach and F. Henry, *J. Electroanal.. Chem.*, 54 (1974) 361.
19. C.Gavach and B. D'Epenoux, *J. electroanal Chem.*, 55 (1974) 59

20. C. Gavach, B. D' Epenoux and F. Henry, *J. Electroanal. Chem.*, 64 (1975) 107

21. D. Homolka, Le Q. Hung, A. Hofmanova, M.W. Khalil, J. Koryta, V. Marecek, Z. Samec, S.K. Sen, P. Vanysek, I.Stibor, *Anal. Chem.*, 52 (1980) 1606.

22. Z. Samec, V, Marecek, J. Koryta and M.W. Khalil, *J. Electroanal. Chem.*, 83 (1977) 393.

23. Z. Samec, V. Marecek and J. Weber, *J.Electroanal. Chem.*, 100 (1979) 841.

24. J. Koryta, P. Vanysek and M. Brezina, *J. Electroanal. Chem.*, 67 (1976) 263.

25. J. Koryta, P. Vanysek and M. Brezina, *J. Electroanal. Chem.*, 75 (1977) 211.

26. Z. Samec, V. Mareced, J. Weber and D. Homolka, *J. Electroanal. Chem.*, 99 (1979) 385.

27. P. Vanysek, *J. Electroanal. Chem.*, 121 (1981) 149.

28. B. Huandhammer, T. Solomon and B. Alemayehu, *J. Electroanal. Chem.*, 135 (1982) 301.

29. B. Hundhammer, T. Solomon and H. Alemu, *J. Electroanal. Chem.*, 149 (1983) 179.

30. A.J. Parker, *Chem. Revs.*, 69 (1969) 1. *Chem. Abstr.* 69 (19690 30649K.

31. O. Popovych, *Crit. Rev. Anal. Chem.*, 1 (1970) 73. *Chem. Abstr.* 75 (1971) 133680S,

32. Z. Samec, D. Homolka, V. Marecek and L. Kavan, *J. Electroanal Chem.* 145 (1983) 213.

33. Z. Samec, V. Marecek and D. Homolka, *J. Electromal Chem.* 158 (1983) 25.

34. B. Hundhammer and T. Solomon, *J. Electroanal Chem.* 157 (1983) 19.

35. P. Vanysek , "Electrochemistry on Liquid /Liquid Interfaces" Spinger-Verlag, Berlin , 1985.

36. Z. Kiczorowski, *J.Electroanal Chem.*, 127 (1981) 11.

37. H.H.J. Girault and D.J. Schiffrin, *Electro chim. Acta.*, 31 (1986) 1341.

38. Z. Koczorowski and G. Gebelewicz, *J. Electroanal. Chem.* 108 (1980) 117.

39. M.H. Abraham and A.F. Danil de Namer *J. Chem. Soc. Faraday I* 72 (1976) 955.

40. A.J. Parker, *Electrochim. Acta.* 21 (1976) 671.

41. T. Solomon, H. Alemu and B. Hundhammer *J. Electroanal. Chem.*, 169 (1984) 303.

42. O. Valent, J. Koryta and M. Panoch, *J. Electroanal. Chem.*, 226 (1987)21.

43. S. Kihara, M, Suzuki, K. Maeda, K. Ogura and M. Matsui, *J. Electroanal. Chem.*, 210 (1986) 147.

44. T. Solomon, H. Alemu and B. Hundhammer, *J.Electroanal. Chem.*, 169 (1984) 311.

45. Z. Koczorowski, J. Paleska and G. Geblelwicz, *J. Electroanal. Chem.*, 164 (1984) 201.

46. A. Sabela, J. Koryta and O. Valent , *J. Electroanal Chem.*, 204 (1986) 267.

47. Z. Samec, D. Homolka, and V. Marecek, *J. Electroanal Chem.*, 135 (1982) 265.

48. P Vanysek , W. Ruth and J. Koryta , *J. Electroanal. Chem.*,148 (1983) 117.

49. D. Guo, J.Koryta, W. Ruth and P. Vanysek, *J.Electroanal Chem.*, 159 (1983) 413.

50. E ,Makrilk, Le Q. Hung and A. Hofmanova, *Electrochim. Acta*, 28 (1983) 847.

51. A Hofmanova, Le Q. Hung, and W. Khalil, *J Electroanal. Chem.*, 135 (1982) 257.

52. J. Koryta, D.Guo, W. Ruth and P. Vanysek, *Faraday Disc. Chem., Soc* 77 (1984) 209.

53. Z. Yoshida and H. Freiser *J. Electroanal. Chem.*, 179 (1984) 31.

54. J. Koryta, Yu. N. Kozlov and M. Skalicky, *J. Electroanal. Chem.*, 234 (1987) 355.

55. D. Homolka, V.Marecek, Z.Samec, O.Ryba and *J. Electroanal chem.*, 125 (1981) 243.

56. D. Homolka, K. Holub and V. Marecek, *J. Electroanal. Chem.*, 138 (1982) 29.

57. C.J. Pedersen, *J. Am. Chem. Soc.*, 89 (1967) 7017.

58. C.J. Pedersen, *J. Am. Chem. Soc.*, 92 (1970) 386.

59. C.J. Pedersen, *J. Am. Chem. Soc.*, 92 (1970) 391.

60. J.M. Kolthoff, *Anal.Chem.*, 51(5) (1979) IR.

61. J.Koryta, Anal. Chim. Acta., 111 (1979) 1.

62. J. Kakwchi and M. Senda, *Bull. Chem. Soc .Jpn.*, 57 (1984) 1801.

63. B. Hundhammer, H.J. Seidlitz, S. Becker and S.K. Dhawan, *J. Electroanal. Chem.*, 180 (1984) 355.

64. B. Hundhammer, S. Becker and H.T. Seidlitz, *Anal. Chem. Symp. Ser.*, 22 (1985) 469.

65. T. Kakiuchi, I. Obi and M. Senda, *Bull. Chem. Soc. Jpn.*, 58 (1985) 1636.

66. T. Osakai, J. Kakutani and M. Senda, *Bull. Chem. Soc. Jpn.*, 57 (1984) 370.

67. T.Osakai, H. Shimoi, T, Kakutani, T. Ohkouchi and M. Senda, *Bull. Chem. Soc. Jpn.*, 58 (1985) 2626.

68. V. Marecek and M. Janchenova, *J. Electroanal. chem.*, 217 (1987) 213.

69. B. Hundhammer and S. Wilke, *J. Electroanal. Chem* 266 (1989) 133.

70. B. Hundhammer, S.K. Dhawan, A. Bekele and M.J. Seidlitz, *J. Electroanal.Chem.*, 217 (1987) 253.

71. J. Yamada and H. Matsuda, *J.Electroanal. Chem.*, 44 (1973) 189.

72. H. Glaurt, *J. Fluid Mechanics* 1 (1956) 625.

73. H. Matsuda, *J. Electroanal. Chem.*, 16 (1968) 153.

74. H. Matsuda and J. Yamada, *J. Electroanal. Chem.*, 30 (1971) 261.

75. D.T. Chim and C.H. Tsang, *J. Electrochem. Soc.*, 125 (1978) 1461.

76. B. Fleet and G. Little, *J. Chromatogr. Sci.*, 12 (1974) 747.

77. W.J. Albery and C.M.A Brett, *J. Electroanal. Chem.*, 148 (1983) 201.

78. H. Gunasignham and B. Fleet, *Anal. Chem.*, 55 (1983) 1409.

79. J.M. Elbicki, D.M. Morgan and S.G. Weber, *Anal. Chem.*, 56 (1984) 978.

80. D.T. Chim and R.R. Chandran, *J. Electrochem. Soc*, 128 (1981) 1904.

81. S. Prabhu and J.L. Anderson, *Anal. Chem.*, 59 (1987) 157.

82. P.L. Meschi and D.C. Johnson, *Anal. Chim, Acta.*, 124 (1981) 303.

83. A.G. Fogg and A.M. Summan, *Analyst*, 109 (1029) 1984.

84. G. Gerhardt and R.N. Adams, *Anal. Chem.*, 54 (1982) 2618.

85. J. Ruzicka and E.H. Hansen, *Anal.Chim. Acta.*, 78 (1975) 145, *Chem. Abstr.*, 83 (1975) 172065e.

86. F.M. Karpfen and J.E.B Randles, *Trans. Faraday Soc.*, 49 (1953) 823.

87. F.E. Powell and A.G Fogg, *Analyst*, 113 (1988) 483.

88. P. Delahay, "New Instrumental Methods in Electrochemistry" Inter Science, New York, 1980 p.228.

89. R.N Adams, "ElectroChemitry at Solid Electrodes." Marcel Decker, Inc. New York, 1969 p.46.

90. R. Kalvoda, "Operational Amplifiers in Chemical Instrumentation" Ellis Horwood ,Chichester, 1975,p.126.

91. L.M Faulkemberry, "An Introduction to Operational Amplifiers." John Wiley , New York, 1977, p.193.

92. N.W, Tietz, "Fundamentals of Clinical Chemitry" W.B Saunders Company, Washington, 1982, p.873

93. A.L. Latner, "Cantarow and Tramber Clincal Biochemistry" 7th Edition, W.B. Saunders Company, Washington, 1975. p.368.

94. J.M. Elbicki, D.M. Morgan and S.G.Weber, Anal. Chem., 56 (1984) 1978.

95. Analytical Method Committee, *Analyst*, 112 (1987) 199